AN INTEGRATED PROPULSION-LIFTING SURFACE SYSTEM FOR HIGH MACH NUMBER OPERATION

by

J. R. BARNARD

June, 1958

AN INTEGRATED PROPULSION-LIFTING SURFACE SYSTEM FOR HIGH MACH NUMBER OPERATION

SUMMARY

Consideration of the various factors which determine the performance of supersonic aircraft and missiles utilizing air-breathing power plants has clearly indicated a critical necessity for optimizing the propulsion system-airframe relationship. Studies of this relationship demonstrate the dominant effects of the required intake and exhaust areas in establishing the airframe configuration for high Mach number cruising flight. In the flight Mach number range from 2.5 to 5.0, it is mandatory to consider the power plant as an integral part of the aircraft from the standpoint of vehicle lift and drag and balance and, in addition, to give careful attention to preserving the maximum possible intake efficiency.

This proposal deals with an integrated ramjet - lifting surface combination which is intended to optimize the power plant - airframe relationship mentioned above. The essential features of the system are:

(a) A variable configuration diffuser

(b) A constant diffuser throat area and Mach number

(c) A constant burner inlet Mach number

(d) A variable exit nozzle

The preliminary analysis contained demonstrates theoretically that the proposed system is feasible. The particular system proposed offers the dual advantages of high design point performance while permitting efficient off-design operation

over a wide Mach number range. The preliminary analysis establishes a number of significant advantages characteristic of this system in addition to the foregoing benefits. The more important of these include:

(a) Increased thrust to drag ratio per pound of payload (particularly at high flight Mach numbers).

(b) Decreased thrust specific fuel consumption for a specific mission and payload.

(c) Structural gains in the form of increased maneuver load capabilities and improved flutter characteristics with no associated weight penalty.

TABLE OF CONTENTS

This study was undertaken as a thesis project to satisfy, in part, the requirements for a Master of Science Degree in Aeronautical Engineering at the University of Michigan, Ann Arbor, Michigan, September 1957 - June 1958.

The author wishes to acknowledge his indebtedness for the council and assistance of Professor D. E. Rogers, of the University of Michigan in the preparation and presentation of this study.

AN INTEGRATED PROPULSION-LIFTING SURFACE SYSTEM FOR HIGH MACH NUMBER OPERATION

PROBLEM BACKGROUND AND GENERAL APPROACH

The ever increasing demands for speed have forced a three-way compromise between a thin low drag wing, a wing capable of withstanding high maneuver loading, and a light wing easy to design and manufacture. This has necessitated increased power and increased demands on target detection and guidance equipment since the course must be planned at greater distances to avoid high maneuver loads. This in turn spells greater weight and a vicious cycle is begun with increased cost, materials, and manufacturing skill required at every turn. Integration of wing and engine design seemed to offer the best design approach for solution of this problem.

This integration of wing and engine design represents a departure from the usual "glider plus power plant" method of design; but the reasoning of L. F. Nicholson[1*] and others seems to indicate that closer integration is a natural design evolution as higher and higher speeds are considered. This reasoning is paraphrased below:

Considering the speed range from Mach 0.8 to 4.0, the most efficient aspect ratio decreases as speed increases. The area required for the air intake, on the other hand, increases quite rapidly. Considering the frontal area of the Mach 0.8 airplane with its large wing span, it was quite reasonable to place the

---

*The superscripts refer to the authors as numbered in "References".

relatively small air intakes and engines rather arbitrarily on a "glider" design. In the Mach 4.0 airplane, however, the situation is reversed and it is quite possible that the best design approach might be to "hide" as much as possible of the body and/or relatively short wing span behind the air intake.

In this design proposal the attempt has been made to "hide" the wing behind the intake. This was done so the wing could be thickened and thus strengthened without adding high drag losses. In the Mach 3.0 to 5.0 flight speed range being considered the choice of a ram jet engine was indicated from the operating characteristics of the various types of engines. "Splitting" or ducting a thin airfoil and placing a ram jet engine in the wing offered many advantages. If the hypothesis is accepted that the most efficient method of providing a strong wing is to thicken the cross-section; then the question of what should be placed inside the thickened wing, fuel or engine, arises. Wing fuel storage is not efficient from the frontal area viewpoint because of the rectangular area cross-section and the need for baffles. The wing structural members tend to require compartmented tanks which increase plumbing, gadgetry, and the possibility of unbalanced wing loading due to trapped fuel. On the other hand wrapping fuel tanks around the engine in the fuselage meets with combat objections.

This thickening of the wing would, of course, greatly increase drag. However, this drag increase can be avoided in large measure, and further weight and drag reduction realized if the engine is removed from the fuselage and placed in the wing. Since the engine intake duct would occupy a portion of the frontal area, depending on the flight speed being considered, the small

slopes and corresponding low drag of the original thin airfoil are largely preserved. Air intake flow also should be considered. The intake ducts should be no longer than the length required to efficiently diffuse the air, and the exhaust area should be of the same order of magnitude as the intake area.* An engine in the wing should reduce this intake and exhaust ducting to the minimum.

In the NACA publication prepared for the 1957 Triennial Inspection of the Lewis Flight Propulsion Laboratory there is an excellent presentation of the drag versus flight Mach number of a hypothetical airplane compared to the thrust available characteristics of the jet engine. The results of the general analysis demonstrate that fixed engine geometry thrust is inadequate, a fixed exhaust nozzle is inefficient, and a variable inlet is required to avoid adverse drag effects from a spillage pattern; for the operation in the Mach range 0 to 4.0. The charts presented in this publication are reproduced in general detail below:

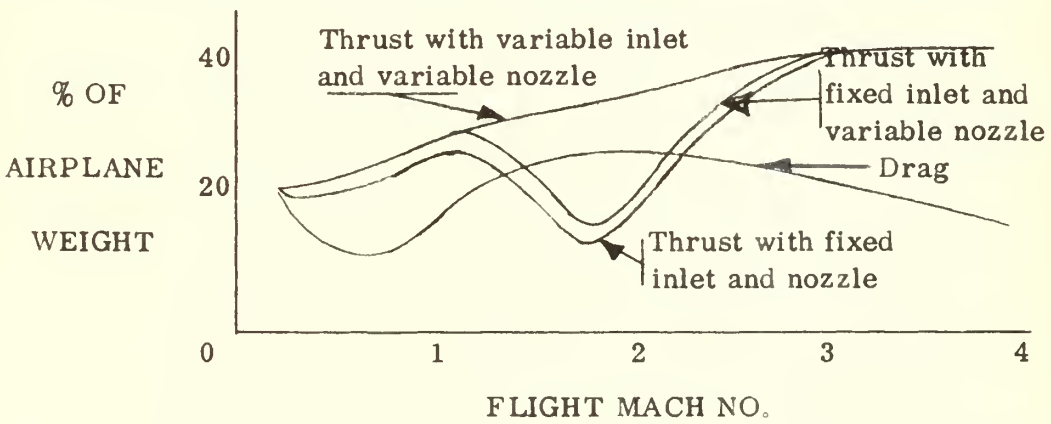

If the integrated wing and engine is to operate efficiently throughout the Mach range, then, a variable inlet and exhaust is required.

A cylindrical geometry offers increased total pressure recovery for a given free stream Mach number, but the mechanics of providing a variable

---

* ref. 1 brings this out particularly well in the author's opinion, and also contains a good discussion by other members of the Royal Aeronautical Society.

geometry while maintaining this increased efficiency lead to overlapping plates and "eyelids"; and the whole system is difficult to design, manufacture, and maintain. Variability in two dimensional flow, on the other hand, can be provided quite simply with light materials easy to manufacture and maintain. In addition, the mechanics of a variable cylindrical configuration might well compromise the higher theoretical pressure recovery by small interferences to flow, over overlapping plates for example, and thus make the actual pressure recoveries of the two systems about equal. If the engine is allowed to extend throughout the span of the wing, an ideal means is provided for accomplishing the required area variations.

This study considers the integration of the components indicated above. The feasibility of such an integration and the inherent low drag, fuel consumption and weight will be demonstrated by considering the performance of the individual components; and by calculating the performance of a specific configuration, the schematic of which is shown on the next page. The ability of the system to withstand high maneuver load while affording a drastic decrease in weight will be demonstrated by comparison to a more conventional design.

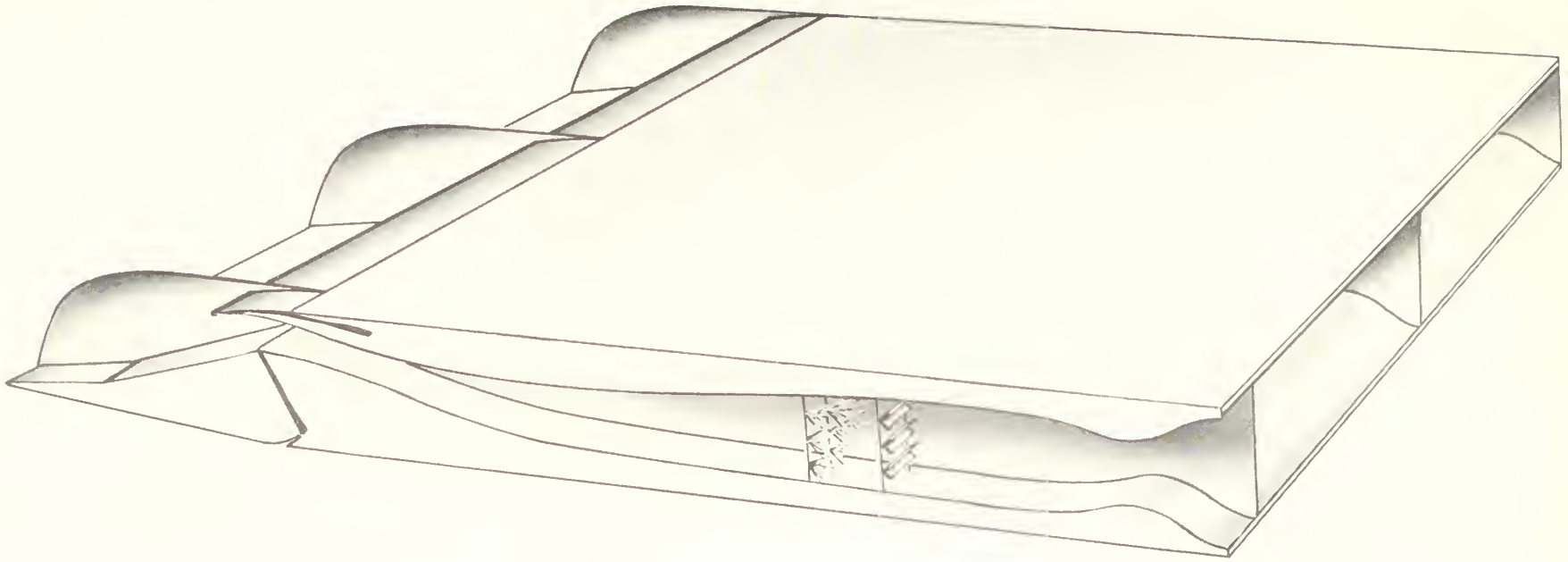

Schematic Wing Section

Two Shock System

$M_{DP} = 3.0$

PROPOSED SYSTEM

Propulsion System

The basic features of the proposed system which offer significant performance advantages are:

(a) a constant inlet throat area, with choked flow;

(b) a constant burner inlet Mach number;

(c) a variable area exhaust nozzle.

This seemed logical from the design objectives since the subsonic diffuser and burner efficiency could thus be maximized and the burner design simplified. The system proposed employs an Oswatitsch type diffuser to slow the flow partially, an "isentropic" diffuser to reduce the flow to Mach 1.0, the previously mentioned constant throat and burner, and a choked flow variable exit. These will be considered in order.

The Supersonic Diffuser

In the first part of the supersonic diffuser a shock wave pattern is formed by the two wedges that make up the shock generator; and external compression takes place, followed by "isentropic" internal compression to Mach 1.0. Since only two large shocks are used in the external compressor, there is a loss in efficiency over the ideal completely "isentropic" diffuser. However, by accepting this initial loss, three advantages are gained. They are:

(1) A smaller initial capture area is required to provide full flow in the throat. This occurs because of the following: Assume that a pure "isentropic" diffuser were used throughout the supersonic flow. Since losses would be reduced, the capture area would have to be increased to provide full flow for

a given size throat. If the burner cross-section is to remain the same, this would require large flow expansion angles on the outside of the diffuser lips at high speed and thus greatly increase the drag. If the burner cross-section is increased to reduce these angles, the drag near Mach 1.0 is greatly increased. If on the other hand, the duct required is shortened to a minimum by using only one or two oblique shocks and a finite strength normal shock, the external compression limits would be exceeded or else high losses will be suffered across the normal shock. In either case compromising losses would be suffered.

It is indicated, therefore, that some loss must be accepted; and the shape of the supersonic compression curves, as well as comparative losses across the normal shock, and space and weight requirements strongly suggest acceptance of loss in the high supersonic flow region.

(2) A shorter duct is required with less boundary layer, drag, weight, and complexity.

(3) An "isentropic" diffuser required a zero angle leading edge. It will be shown later that the angle required for the leading edge for a design speed of Mach 3.0 is approximately ten degrees. It was felt that this angle could be realized in manufacture and would have sufficient strength to retain its shape in flight.

The use of external compression offers a great advantage by reducing the throat area necessary for swallowing the shock when starting the engine. This normal shock will be present at the forward part of the lip at the entrance to the internal supersonic "isentropic" diffuser when the engine is not producing thrust, due to the difference in flow conditions between an engine that is producing

thrust and a cold engine. When the engine is started this normal shock will be swallowed (move aft of the throat) and then be forced up to the throat by the action of the variable exit nozzle that will be discussed later. The fact that the capture area is variable permits easy starting of the engine, and allows the engine to operate at peak efficiency since the ratio of the capture area to the constant throat area can be changed from that required for swallowing to that required for peak efficiency. A schematic cross-section of the proposed system is given on the next page.

The Subsonic Diffuser

Ref. 8 gives the relation of total pressure recovery to the rate of change of the cross-sectional area per foot of length of a subsonic diffuser. It can be seen that this curve peaks quite sharply and has a definite maximum. Since the diffuser throat area and burner area are kept constant, the subsonic diffuser can be designed to realize this peak efficiency for all values of free stream Mach number. This, of course, would not be possible without some difficulty if the throat area were allowed to vary.

The Burner and Exhaust System

Because of the constant burner Mach number, the burner design can be simplified for low cost and ease of maintenance and optimized for peak efficiency; and this efficiency will be maintained for all values of free stream Mach number.

A two dimensional variable exit is proposed (see Fig. 7) to accelerate the flow to the local speed of sound at the throat (choked flow) and provide expansion of the flow to ambient pressure. This makes the engine easier to control and, as will be shown in the calculations, increases the thrust as much as 60%. Because of the large thrust to drag ratio, particularly at high speed and high altitude, of

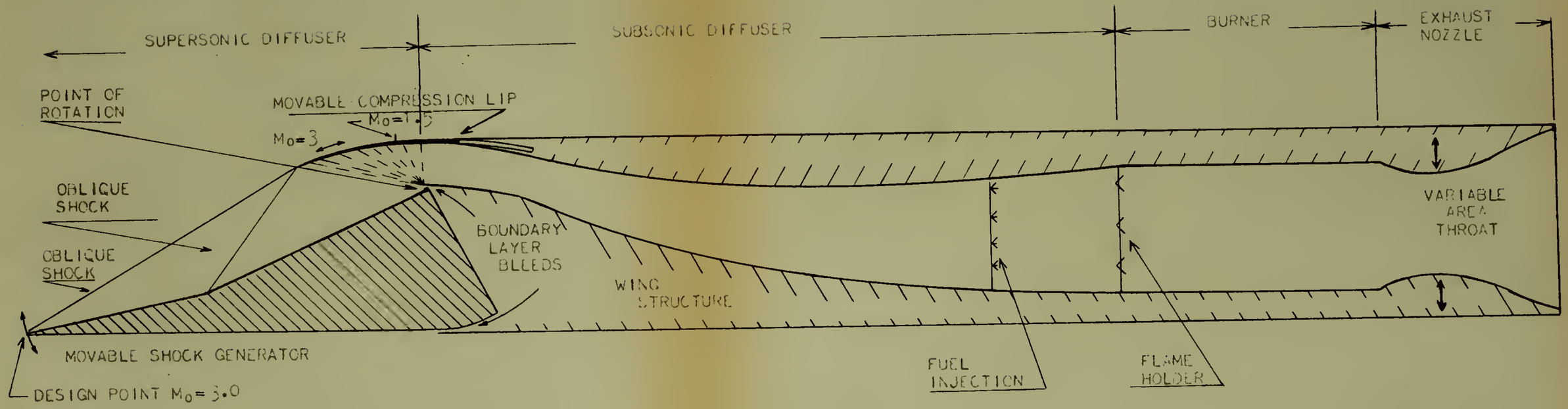

SCHEMATIC OF PROPOSED

RAMJET-LIFTING SURFACE SYSTEM

the proposed wing engine combination; cruise will be at reduced throttle. The throat will have to close further under this condition to maintain choked flow. At some point, then, the variable throat will be positioned so that the exit area to throat area ratio is optimum and ideal expansion will result with greatly increased thrust. The improvement in performance that is present over the entire speed range will be greatest at this point.

Lifting Surface

It will be shown later that for best total pressure recovery when operating below the design speed, the shock generator must be rotated up. This rotation places the outer surface of the shock generator at some angle to the relative wind. It was found that the lift produced from this free stream deflection could provide the lift required for level flight at moderate altitudes while the total pressure recovery of the inlet air was kept at or near the maximum. This is not the best way to produce lift, dragwise, since it involves larger angles over shorter chord lengths. It is, however, a very efficient method when air intake and compression is also considered, because of the double use of the shock generator. The relative efficiency of "by passing" some of the air not required for engine operation at below design speed, converting it to lift, and accepting the relatively high drag versus allowing the excess air to enter the intake and then trying to dump it with as little loss as possible will be discussed later. Structural benefits that also accrue from this action will be discussed in the next section.

Structure

For structural purposes the usual supersonic wing is only considered in the area between 25% and 75% of the chord since the pointed leading and

trailing edges outside of this area provide so little resistance to bending that their vertical load supporting capabilities are negligible. With the system proposed, however, the effective moment arm is available over an increased portion of the chord. This provides an increased load carrying capability of the wing that is further increased because the full maximum thickness of the normal wing can not be used as a moment arm, even between 25% and 75%, because of upper and lower wing surface curvature.

Even a greater margin of strength is provided, however, by the large increase in wing thickness and thus moment arm. The recent design problems and special manufacturing techniques are thus avoided, and wing design is reduced to standard techniques where a great deal of background data is available. Even considering the additional weight of the engine inside the wing, this wing is easier to design and manufacture, lighter, and capable of supporting more vertical load than the normal thin supersonic wing. This is particularly advantageous for high altitude intercept since it reduces the requirements on intercept angle, flight path, detection equipment, and computer equipment; and takes the latter two items out of the long range radar and crystal ball category. Due to the lessened requirement or intercept angle, early warning detection requirements are reduced since an intercept is possible by flying in the direction of the target instead of going around behind and overtaking. This shortens the flight path and reduces time and weight requirement.

Aeroelastic effects that cause the wing to twist when an aeleron or other control surface is deflected are greatly reduced because of the enlarged "torque box" (increased wing thickness and usable chord length) that is available. The

elastic deflection when high maneuver load is applied is greatly reduced as previously mentioned. Therefore aeroelastic effects weren't considered.

The effects of inertia coupling were not computed, but it can be seen that the thickening of the wing and the reduction in size and weight of the fuselage will give a much more favorable mass distribution. The proposed system has been partitioned by solid ribs in order to support the skin and stringers, eliminate any transverse wave formation, and, by extending these ribs forward, to provide a secondary means of supporting and positioning the shock generator and compressor lip. This is shown on the oblique view previously given in the "Problem Background" section.

The structural load on the compressor lip of the proposed system is not as great as might be imagined. The outside of the lip is inclined to the relative wind; therefore, there is a pressure force behind the shock wave it creates that tends to push the lip in. The intake flow that has been compressed by the shock generator tends to push the lip out. At the leading edge of the compressor lip these two forces will nearly balance each other and result in a small moment even though the moment arm is relatively long. As the compressor lip turns the flow, the pressure pushing the lip out will begin to dominate the force balance; but at the same time the moment arm will be decreased and thus a relatively low moment will be maintained.

If this pressure balance were ignored, one might well attempt to decrease the drag of the system by somehow making the outer surface of the compressor lip parallel to the free stream. However, from the above it can be seen that this would force a drastic increase in moment on a member that must be kept

thin for best efficiency. Therefore, the net result of this attempt might well be a loss in net thrust (thrust minus drag) through loss in compression efficiency as well as an increase in weight.

This balance of pressure forces also works to advantage in the case of the shock generator when it is positioned for operation below the design speed. Here again the outer surface is inclined to the relative wind and the inner and outer pressure forces tend to balance each other.

SYMBOLS

A	area (feet^2)
b	wing span (feet)
C	Dimensionless coefficient, also wing structural chord
c	wing chord (feet)
C_F	thrust coefficient based on dynamic pressure
C_f	exhaust thrust coefficient
D	total drag (pounds)
d	the couple moment arm to resist wing bending
d_H	hydraulic diameter (feet)
F	thrust (pounds)
g	acceleration due to gravity (32.2 feet/sec^2)
K	thousands (10K is ten thousand)
L	total lift (pounds)
M	Mach number
p	pressure (pounds/feet^2)
P_{T_1}/P_{T_O}	total pressure recovery ratio of the supersonic diffuser
R	body radius (feet)
S	wing area (feet^2)
S. L.	Sea Level
T	temperature (^{O}R) degrees Rankine
V	velocity (ft/sec)
W	airplane weight (pounds)
$\dot{w}$	engine mass flow (pounds/sec)

Greek leters

α angle of attack (degrees)

β angle of the shock wave relative to the flow in front of the shock (degrees)

γ specific heat ratio

η efficiency factor

θ wedge angle of flow deflection (relative to the flow in front of the wedge) (degrees)

ν angle of deflection of Prandtl-Meyer "flow around the corner" (degrees)

ϵ exhaust exit area versus throat area ratio

Subscripts

0 free stream conditions

1 conditions after the first shock in the diffuser when considering the diffuser only, and at the diffuser throat when considering the complete engine.

2 conditions after the second shock in the diffuser, and at the entrance to the burner when considering the complete engine

3 conditions after the third shock wave, and at the exit to the burner

D drag

DP design point of the diffuser

e exit conditions at the exhaust nozzle

L lift

N Normal shock

T stagnation or total pressure (P_{T_O} is the stagnation free stream pressure) (pounds/feet^2) also the exhaust nozzle throat conditions.

W wedge angle relative to free stream intake flow when the shock generator is positioned for some Mach number other than M_{DP} (degrees)

ANALYSIS

The analysis of this proposal has been divided into two parts; the outside of the wing and engine system, to include aerodynamic and structural considerations; and the inside, or ducted area, to include the supersonic diffuser scheme and engine considerations. The thickness of the overall wing was fixed by the required capture area of the air intake which is in turn dictated by the throat height. The chord of the wing was fixed by the following factors:

(a) the required length of the shock generator or supersonic diffuser

(b) the length required by the subsonic diffuser so as not to exceed efficient diffusing rates

(c) the length required for the burner

(d) the length required for the variable exit

By expressing the burner length and exit length in the customary burner diameters (in this case burner height) it can be seen that the chord length is also dictated by the throat height, if the burner Mach number and thus area is kept constant.

In this section only the drag and thrust per span foot of wing will be considered. It will be further assumed that the wing has a constant cross-section A diffuser throat height of two inches was arbitrarily chosen. Since all wing cross-section dimensions are based on this throat height, all dimensions were specified. This made the actual chord:

Shock generator	1.625 ft.	.271 Total chord
Aft wing	4.375 ft.	.729 Total chord
Total chord	6.000 ft.	1.000

The height of the throat is limited by the length of the generator that can be controlled and held in place, but 1.625 feet seemed very reasonable. Using the optimum diffuser configuration that will be determined for M_{DP} 3.0 the performance of one spanwise foot of wing was determined by the calculations as shown in Appendix I and II. The method of calculation used and the assumptions made will be discussed in order.

Determination of Optimum Supersonic Diffuser Configuration

In the original theoretical analysis of this type of diffuser by K. Oswatitsch[2] it was found that the maximum total pressure recovery through n-1 oblique shocks and one normal shock is accomplished by making the total pressure ratios across all of the oblique shocks and the normal shock equal. This criteria will be used to find the strength of the two oblique shocks for optimum performance of the first portion of the supersonic diffuser. The second portion of the supersonic diffuser employs "isentropic" compression. "Isentropic" has been placed in quotation marks thus far to denote that there are some losses in the compressor and thus the flow is not actually reversible. These losses will be discussed later and shown to be small, thus the flow does approach the isentropic condition. This flow is actually Prandtl-Meyer flow around a corner or zero radius turning. Parameters for this flow can be found in any good aerodynamics book.[3]

The flow through the diffuser throat is parallel to the free stream flow. Therefore, the angle of deflection of the Prandtl-Meyer flow is equal to the total angle of deflection of the flow caused by the two oblique shocks (see Fig. 1). Prandtl-Meyer flow deflected through some angle has a unique Mach number. By considering the flow to be compressive instead of the normal expansive flow,

this unique Mach number will be the Mach number before deflection. Parameters for this type of flow (diffuser shape, focal point, etc.) are given in TN 3589[4] and have been confirmed by experimental results. Matching this unique Mach number of the flow before Prandtl-Meyer deflection to the Mach number of the flow after the two oblique shock deflections by iteration, and using the Oswatitsch criteria for equal total pressure losses across the two oblique shocks gives a unique optimum configuration for diffusing any given free stream Mach number to sonic velocity. Fig. 2 gives; as a function of the free stream Mach number, M_o; this optimum configuration in terms of θ_1, the first wedge angle of deflection to the free stream; M_1, the Mach number of the flow after deflection through θ_1, degrees; θ_2, the second wedge angle of deflection to the previously deflected flow; M_2, the Mach number of the flow after the second deflection; ν, the total angle of oblique shock deflection equal to the deflection angle of the Prandtl-Meyer flow; β_1, the generated shock wave angle relative to free stream M_o; and β_2, the generated shock wave angle relative to the flow after the deflection by θ_1. These values were taken from charts.[5] By applying the condition that the two shock waves intersect at the isentropic diffuser lip, a unique configuration is specified by some given throat height. Fig. 1 was constructed, as an example, for a optimum diffuser of M_o 3.0 flow where the throat height was taken as one inch. This configuration of the shock generator is, therefore, defined as Mach Design Point for a free stream Mach number of 3.0, M_{DP} 3.0. Considering only the optimum configuration for each free stream Mach number as given in Fig. 2 (M_{DP} and thus the configuration changing), the total pressure recovery ratio between the free stream and the diffuser throat was computed from charts[5] to give the maximum

theoretical total pressure recovery for the proposed configuration at any given M_{DP}. The results are given in Fig. 3 for a two oblique shock system. The improved performance of a three shock system will be given later.

Design speed pressure recovery curves, adjusted for losses as discussed in Appendix III, have also been included in Fig. 3 for optimum configurations using three oblique shocks plus one normal shock, two oblique shocks plus one normal shock, and one oblique shock plus one normal shock. Comparison of these curves show the proposed design to be superior at design speed, M_{DP}.

The Constant Configuration Shock Generator

If the optimum configuration for some M_{DP} is taken, and a constant configuration shock generator constructed and rotated about the point at the focal point of the isentropic compressor (Point A in Fig. 4), a unique position of the shock generator relative to free stream may be determined in the following manner:

At some rotated position of the shock generator the outer surface of the shock generator will form some wedge angle relative to the free stream, θ_o. The parameters of this outer or by-passed flow will be discussed later. The inner surface of the shock generator will also form some wedge angle relative to the free stream intake flow, θ_w. Since the shock generator configuration is constant:

$$\theta_o + \vartheta_w = \theta_1 = \text{constant}$$

$$\vartheta_2 = \text{constant}$$

$$\theta_w + \vartheta_2 = \nu$$

For some given ϑ_w, M_1 is specified and, since ϑ_2 is constant, M_2 and ν are

also specified. By iteration to match M_2 and ν to the Prandtl-Meyer flow characteristic Mach number and angle of deflection, a unique position of the shock generator can be determined for any given free stream Mach number. This of course requires that the isentropic compressor be retractable, since a different deflection angle is required for each M_o. The isentropic compressor lip, then, is a preformed member that is retracted into a channel as controlled by the same free stream Mach number sensing device that controls the position of the shock generator. The isentropic compressor profiles given in ref. 4 demonstrate that this constant shape of the lip is possible over the range of M_2 being considered ($M_2 < 2.22$). The advantages of this movable lip have been mentioned previously and will be discussed in more detail later, as will the structural considerations. This scheme of operation is shown schematically in Fig. 4 where the position of the leading edge of the lip is noted by the number corresponding to the free stream Mach number, M_o.

Operation of this configuration below design speed will result in slightly less than the given $P_{T_1/P_{T_o}}{}_{max}$ pressure recoveries. To demonstrate the magnitude of this loss, the same design speed originally taken of M_{DP} 3.0 was again selected. The theoretical pressure recovery curve of this configuration is shown in Fig. 5 and labeled "Constant θ_1 and θ_2' for M_{DP} 3.0. It can be seen that this performance is slightly less than the maximum possible for Mach numbers less than 2.0 of other configurations when they are operating at design speed, but is superior from there to beyond design speed. The AIA Ram Recovery Curve has also been included for comparison. Fig. 5 shows the loss in total pressure recovery as compared to $P_{T_1/P_{T_o}}{}_{max}$ for operation at speeds below M_{DP}.

The partial external compression and partial internal compression provided avoids the flow deflection problem at the exterior of the isentropic compressor lip and allows the lip to have a finite angle at the leading edge without causing a detached bow wave and the accompanying spillage and drag. This can best be seen by noting that slightly subcritical flow is easier to control and increases pressure recovery characteristics slightly. Therefore, best operating conditions would move the shock waves caused by the shock generator slightly forward of the critical flow condition shown in the figures. With this shock pattern moved forward it can be seen that the isentropic compressor lip lies entirely within the deflected flow caused by the shock generator. The leading edge angle of this lip can, therefore, be made some small angle without producing a detached bow wave.

Boundary Layer Considerations

As shown in Fig. 6, it is assumed that the boundary layer will begin to build on the inner surface of the shock generator. This layer will tend to pull away from the surface as it nears the flow pattern caused by the isentropic compressor lip. The ducting at A is such that it scrapes off a portion of that layer before the pull away tendency becomes pronounced. The boundary layer scraped off is utilized for cooling as described later. The same scheme of scraping off the boundary layer on the outer surface of the shock generator is used at Point B (see Fig. 4). Wind tunnel experimentation has shown that the boundary layer on the isentropic compressor lip can be minimized by holes drilled at an angle in the compressor lip. These holes are positioned so that the number exposed to the flow will be increased in proportion to the tendency

for the boundary layer to grow as the compressor lip is extended.

Subsonic Flow

The flow thus enters the throat (see Fig. 4) with a very small boundary layer at a speed very close to sonic velocity. After the engine is started, a normal shock wave is formed at the throat and kept there by burner and exit conditions that are controlled by the variable exit that will be discussed later. Therefore, choked flow with constant diffuser throat area is maintained at all engine operating conditions. Since the flow change across the normal shock is from very slightly supersonic to very slightly subsonic, a minimum total pressure loss is experienced across this normal wave. The subsonic diffuser losses can be minimized by the use of the optimum expansion angle in the diffuser. Space has been provided to efficiently diffuse the flow to Mach 0.2 at the burner, and a conservative efficiency of .90 was assumed for this operation in the later calculations.

The Burner and Exhaust System

The burner has only been shown schematically. As mentioned previously, a simplified design is possible because the inlet Mach number is maintained constant. In thrust computations it was found to be convenient to use a dimensionless coefficient, C_F, that was computed by:

$$C_F = \frac{T}{\gamma/2\ P_o\ M_\infty^2\ C}$$

where C is the average wing chord and T is the thrust of one lineal foot of wing. These computations were also made in Appendix I and II, and the computed values of C_F are given on Figs. 10 and 14.

Since exit area versus throat area ratio, ϵ, was used to some extent in the calculations, the usual ram jet thrust equation was rewritten as:

$$F = F_e - F_o$$

where $F_e = C_f P_{T_3} A_T$ and $F_o = V_o \dot{w}/g$

values of C_f were then obtained from charts.[7] The area of the exit is limited by the dimensions of the wing. When the optimum ϵ was exceeded (about M_o 2.2) the area of the throat was decreased to make this ratio optimum. This in turn decreased the fuel air ratio for operation well below stoichiometric.

It was found from a determination of C_F that at low supersonic speeds C_F rises with altitude, but this rise is limited by the total temperature rise at stoichiometric fuel ratio (thermal choking) above some optimum altitude. It was assumed that 20,000 feet altitude provided the maximum C_F/C_D ratio. At this altitude the shock generator produces a very large portion of the lift required for level flight as previously mentioned. Only the altitude of 20,000 feet was considered in the low supersonic speed range, since showing thrust to be well over the drag for one altitude demonstrates the ability of the vehicle to accelerate to cruise speed.

Cooling

Cooling is accomplished by the two streams of boundary air bled from Points A and B as previously mentioned. The air from Point A is channeled through hollow posts that make up the middle portion of the front spar as shown in Figs. 4 and 8. This flow is then led aft to cool the compressor lip side of the wing, and exhausted out the rear. Air from Point B is used to cool the shock generator side of the wing. Increasing the size of the wing would increase

the size of these cooling passages accordingly.

Lifting Surface

Since the engine air intake has been located in the leading edge of the wing and accounts for part of the air-stream ahead of the wing, the drag-wise effect of thickening the wing is greatly modified. In order to estimate the magnitude of this effect the dimensionless lift coefficient, C_L, was computed as the lift required for level flight from the formula:

$$C_L = \frac{W/S}{\gamma/2 \; P_o \; M_o^2}$$

where W/S was taken as a constant 200 pounds per square foot; and the dimensionless drag coefficient, C_d, was computed for one foot of wing using a diffuser throat height of two inches, which gives a sectional dimension of the shock generator per 24 square inches of throat area. Refering to the figure below, the curved portions of the upper and lower surfaces (X and Y respectively) were approximated by extending the sloped surface to the intersection with a horizontal line. Since the diffuser has a practically constant orientation with the relative wind, the horizontal portion of the simplified model will have no drag.

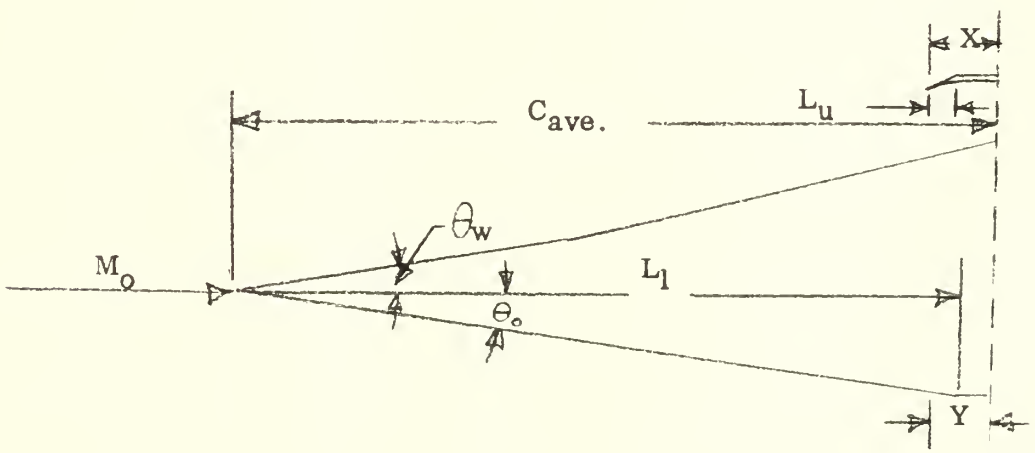

It was felt that this simplification would yield results certainly within the accuracy of the method of linearized thin airfoils used to compute the drag. The outer surfaces of a diffuser for a given M_{DP}, then, have a chord-wise length and slope for both the upper and lower surface that is dependent on M_o. Linearized thin airfoil theory was then utilized to obtain a C_d:

$$C_D = \frac{2}{C_{ave}\sqrt{M_o^2 - 1}} \int_o^L \left[\left(\frac{dy}{dx} \right)_{up}^2 + \left(\frac{dy}{dx} \right)_{low}^2 \right] dx$$

where L is the chord-wise length. It should be noted however, that this C_d is based on an average chord length from the tip of the shock generator to the axis of rotation of the shock generator. When a C_d of the remaining portion of the wing is computed based on its chord, the two chords must be totaled and the two C_d's combined in proportion to their characteristic chord's fractional part of the total chord. Thus if the average chord length of the shock generator for some M_{DP} was 1/4 of the total chord, the total C_d would be:

$$1/4\ C_{d_{(\text{shock gen.})}} + 3/4\ C_{d_{(\text{remaining wing})}} = C_{d_{\text{total}}}$$

A C_L based on linearized thin airfoil theory was also computed that must be combined in the same manner:

$$C_L = \frac{4\alpha}{\sqrt{M_o^2 - 1}} \left(\frac{1}{57.3} \right) \quad (\alpha \text{ in degrees})$$

The above value must be divided by two when computing the shock generator lift, since only one surface is considered. C_L and C_d were computed for the remaining wing by the normal application of linearized thin airfoil theory. The lift of the intake air passing through the engine was assumed to be zero by the following argument: It will be shown later that the aft portion of the wing remains practically constant at zero degrees relative to the free stream. The vertical component

of the momentum flux entering the engine is zero since the free stream is horizontal. If the angle of attack of the aft portion of the wing is zero, then the vertical component of the momentum flux leaving the engine is zero. Therefore, the vertical momentum change and thus the lift must be zero.

Computations were made in Appendix I for a two shock system with M_{DP} 3.0, and in Appendix II for a three shock system with M_{DP} 4.0. In some cases angles greater than the normal limit of accuracy of the formulas were used. However, in each case the proportional part of the total term was considered so that the resultant error was reduced to an acceptable value when considered as an error for the whole term. The computed values of C_d are given on Figs. 9 and 12. The results of these calculations are used as a basis for estimating total drag in order to demonstrate the feasibility of the system.

It can be seen from Fig. 4 that as M_o is decreased; θ_o, the outer wedge angle of the shock generator, is increased. Therefore, there will be a speed at which the shock wave attached to the leading edge of the generator tends to become detached and form a bow wave, with the flow behind this wave subsonic. At this point, if θ_o is decreased slightly, the shock wave will again become attached to the leading edge, but the normal shock will move from the throat to the lip of the isentropic diffuser, since the turning angle inside the diffuser is too great. With the normal shock wave positioned at the lip, it can be seen that the isentropic diffuser is now acting as a normal shock diffuser with the Mach number ahead of the normal shock greater than a slight amount above Mach 1.0. A total pressure loss will now be incurred across the normal shock at the lip.

During this regime (when the leading edge shock wave is kept attached to

the leading edge by decreasing θ_o) C_d and C_L will increase more slowly as M_o is decreased. This retarded increase in C_L will force an increase in C_L for the remainder of the wing to maintain level flight; and some point will be reached, depending on the individual configuration, where C_F / C_D will become a maximum for each M_o. The location of this exact optimum point for each M_o, using theoretical data is rather meaningless, since it involves the difference of relatively large quantities to find a minimum. These exact optimum points are not critical if it can be demonstrated that at each point the thrust is well above the drag and thus the vehicle is capable of acceleration through this region.

In this investigation the position of the generator was arbitrarily chosen as shown in Fig. 9 by the following schedule:

$M_o > 2.2$	Best total pressure recovery (shock in the throat).
$2.2 > M_o \geq 1.5$	Limit of external compression (shock on the lip).

This compression limit is shown on Fig. 9 in terms of M_2 as "M_L". This value was taken from NACA TN 3589. The indicated M_2 in the figure was slightly increased to insure a stable shock system. The position of the shock generator required to produce this shock system is given on Fig. 9 in terms of ϑ_o, M_o less than 1.5 was not investigated because theoretical results in this transonic region have doubtful accuracy, and are properly a case for wind tunnel investigation. Considerations for operation of the compressor at speeds below this region considered above will be discussed later. At this point it suffices to say that for the schedule chosen, no normal shock will form either on the inner or outer surface of the shock generator. Since there will be no shock detachment, no addition drag from intake air spillage will be present.

Structure

In a later section an approximate solution is obtained for the proposed system with a body and tail attached in order to compare the proposal with a conventional vehicle with a supersonic thin air-foil wing.

DISCUSSION

Operating Characteristics

In order to demonstrate the feasibility of the proposal, the previously calculated values of C_d and C_F per spanwise foot of wing were used to obtain the performance of a vehicle using the proposed system. These calculations were also made in Appendix I and II. The resultant thrust and drag coefficients have been plotted versus Mach number for various altitudes in Fig. 10 for the two shock system with M_{DP} 3.0 and in Fig. 14 for the three shock system with M_{DP} 4.0. It can be seen from these plots that the large amount of excess thrust provides excellent maneuverability in a wide operating range that will exceed the altitudes and speed values computed. This large amount of excess thrust will dictate reduced power settings in most cases, so that the burner temperature calculated will probably not be obtained except while operating close to Mach 1.0. The scheme of maneuver here is to traverse this area as rapidly as possible and to avoid this range in the same manner that most aircraft avoid certain operating areas.

The effect of wing moment coefficient was not considered. Wind tunnel tests will probably prove that this configuration can be operated through the transonic region and down in the subsonic region. However, the theoretical calculations required for sufficient accuracy in these areas are beyond the scope of this proposal and the ability of the author. The spanwise length of the wing was fixed by consideration of such factors as the wing loading, the aspect ratio, and the proportional part of the drag caused by body and tail surfaces that each foot of engine would have to account for. Because of the use of

dimensionless coefficients of drag and thrust and the unique relationship of all cross-section dimensions, the C_F and C_D values determined hold for any throat height as long as the wing loading is held constant. Therefore, if the body weight and shape are held constant, the aspect ratio is inversely proportional to the throat height and can be set from considerations of best structural efficiency. A wing loading of 200 pounds per square foot was chosen.

The closed body shape given by Haack[9] was used for these calculations since it has a minimum drag for a given volume and length:

Profile: $R/L = R_{max}/L(x/L - x^2/L^2)^{3/4}$ $\qquad R_{max}/L = .04$

The approximate wave drag of the body is given below:[9]

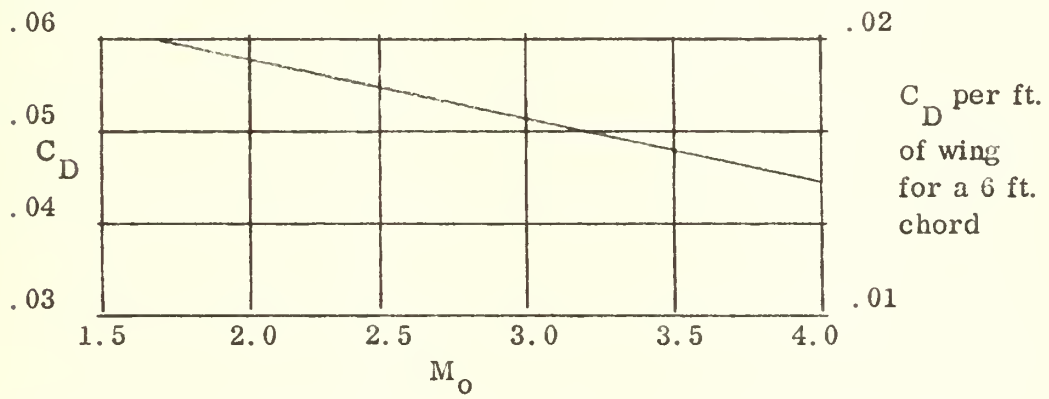

Assume that the drag of the rest of the body and the skin friction of the complete body equals the body wave drag. Assume that $R_{max} = 1.38$ Ft.; the frontal area will then be 6.00 ft.^{2}; and the equivalent frontal area to include the rest of the body and skin friction will be 12.00 ft.^{2}. Referring this to a lineal foot of wing with a chord of six feet will multiply the above C_D value by two. If the length of the wing is taken as six feet, each lineal foot of wing will have to account for 1/6 of the above C_D or 1/3 of the given C_D value. This scale is plotted on the right side of the figure. This gives, on the following page, the values for M_o considered:

M_o	1.5	1.75	2.2	2.6	3.0	3.5	4.0
C_D	.0202	.01975	.019	.0182	.0175	.0165	.0155

It was felt that this was an overly large body and all assumptions conservative. The actual span of the wing will, therefore, be 8.76 feet and the aspect ratio 1.46. It was assumed that the body produced no lift, the vehicle had a gross weight of about 7,500 pounds (300 lb. fuel assumed consumed accelerating to $M_o = 1.5$).

The C_D and $C_{F_{max}}$ calculations shown on Fig. 10 were made using the variable exit nozzle previously discussed. It was assumed that the missile could be rolled 180° (turned upside down) at cruise speed in order to utilize the lift of the isentropic compressor lip at M_o 3.0, and the lift of the shock generator at greater speeds. The probable behavior at speeds between M_o 1.0 and 1.5 has been indicated on the figure in dashed lines, on the basis of typical operation in this region.

The angle of attack was found to remain nearly zero (0° to 6°) for this condition. The condition where the vehicle was restricted from rolling was also investigated. The angle of attack was found to be greater (1.2° to 7.7°) for this case. However, in both cases C_F remained well above C_D as can be seen in Fig. 10. Loss of lift at the wing-tip was not considered. However, since most of the lift is produced at the forward part of the wing, a very small portion of the lift producing surface lies within the wing-tip Mach cone. This loss of lift was, therefore, considered negligible.

Performance of a Three Oblique Shock System with M_{DP} 4.0

A three oblique shock system was investigated for a Mach Design Point of 4.0. The configuration shown on Fig. 11 was taken from the chart on Fig. 12.

Fig. 12 also gives the limiting Mach number for external compression as discussed previously; and the total pressure recovery of the supersonic diffuser, $P_{T_1/P_{T_o}}$, when the diffuser is operating at design speed, M_{DP}. It should be noted that the total pressure recovery is greater than the theoretical maximum for a fixed geometry isentropic diffuser with maximum external and maximum internal compression. This maximum is shown on Fig. 12 as given in ref. 4. Exceeding this curve is possible because of the variable configuration of the proposed design. This can be readily seen by recalling that the external compressor is limited as previously mentioned; and in the theoretical maximum case by the area ratio of the internal compressor entrance to throat area for shock swallowing. This limit does not exist for the proposed design since this ratio can be controlled by moving the small lip.

The schedule for the position of the shock generator for this study was arbitrarily chosen as shown in Fig. 13. It is summarized below:

$M_o > 3.0$	Best total pressure recovery
$3.0 > M_o > 2.0$	Arbitrary schedule (The curves shown on Fig. 12 and 13 could be considerably straightened by selecting the optimum shock generator position.)
$2.0 > M_o > 1.75$	M_3 slightly greater than M_L (the limit of external compression).
$1.75 > M_o > 1.5$	M_2 slightly greater than M_L.

It is previously stated that methods to extend the low supersonic range operation without a normal shock forming either on or in front of the shock generator; and the relative efficiency of "by passing" some of the air in front

of the wing, converting it to lift, and accepting the relatively high drag; would be discussed later. These can best be illustrated by the design now being considered in the Mach 1.5 to 1.75 range. Here it is proposed to hinge the last ramp and make θ_3 zero at speeds below M_o 1.75, as shown in Fig. 11. This allows M_2 to approach M 1.0 without a normal shock forming at θ_3. This is directly applicable to the two shock case by hinging the last ramp there. This positioning device need only be a two position system and can thus be kept small and light. One is tempted to utilize this hinged ramp system at greater speeds, and thus be able to hold the position of the shock generator fixed, and achieve design simplification. Consider, however, the thrust equation:

$$F = \frac{\dot{w}_e}{g} V_e - \frac{\dot{w}_o}{g} V_o \qquad \begin{matrix} p_e = p_o \\ \text{(optimum exhaust expansion)} \end{matrix}$$

The $\frac{\dot{w}_o}{g} V_o$ term increases as the square of the velocity. At low supersonic speed some additional air can be utilized for cooling between the burner wall and wing skin; and then exhausted at the trailing edge to recover this lost thrust. If the variable ramp is attempted exclusively, the passages are no longer capable of handling the large mass flow; and air must be dumped, with an accompanying high loss of thrust.

C_D and $C_{F_{max}}$ calculations were made as before in Appendix II and are given in Fig. 14. The same body shape and dimensions and wing loading were used. It was felt that the increased weight enclosed in the body was more realistic, but still conservative. The height of the diffuser throat was taken as one inch, making the diffuser length 27 inches and the aft wing 27 inches for a total chord of 4.5 feet. The length of the wing was taken as 12 feet, giving a

wing span of 14.76 feet, an aspect ratio of 3.28, and a gross weight of the vehicle about 11,000 pounds. Again it was assumed that the missile could be rolled for cruise. The angle of attack was again found to remain nearly zero (0^{o} to 1.23^{o} at 20,000 feet) for this condition. The effect of restricting this roll was not investigated, since it was shown previously to be negligible. Again C_F remained well above C_D as can be seen in Fig. 14. Wing-tip loss of lift was not considered for reasons previously mentioned. For this design the relative thickness of the wing increased while the relative thickness of the burner remained constant. Increased ϵ ratios were, therefore, possible and a C_f value as high as 1.596 was realized at M_o 4.0.

The basis for determining the span was the requirement of a satisfactory margin of excess thrust for vehicle acceleration in the M_o 1.5 region. If partial boost can be permitted in this range, a further extension of range and/or decrease in weight is possible.

It is shown in Appendix I and II that in both M_{DP} 3.0 and 4.0 cases, α remains very close to zero throughout the operating range considered until cruise speed is reached. If the missile is rolled, α is again very close to zero for both cases in the cruise condition.

Comparison of the Proposed Design to a Conventional Design

Since relative wing strength and ability to withstand high maneuver load will be an important part of the comparison, the conventional configuration selected for comparison should have the engine located on the wing and not in the body. This will remove the body and wing root strength from consideration and allow attention to be focused on the wing itself. To further aid in the comparison,

wing area plan shapes should be the same; that is straight, low aspect ratio wings. To further simplify the problem, consider the conventional engine to be supported on the wing in such a manner that its weight and thrust loads are evenly distributed throughout the length of the wing. If such a mounting were possible, it would certainly be advantageous to the conventional design. Further, assume that, in the proposed configuration, the cooling space between the burner and wing skin and the rate of flow of air in this space are such that the skin temperature of both wings are equal to the aerodynamic heating value for the Mach number being considered. This will avoid consideration of the reduced strength and increased boundary layer growth due to increased skin temperature, since both wings will react the same. The wing selected for comparison was the following:

Wing section	3% biconvex with eliptical nose
Taper ratio	.388
Aspect ratio	3.08
Angle of sweep	0^{o}

No digedral, twist, camber, or incidence

Values of C_D and α were obtained from wind tunnel tests of a wing and body model. Assume the proposed configuration has the following, to more closely match the wing used for comparison:

Taper ratio	1.0
Aspect ratio	3.08
Angle of sweep	0^{o}

No digedral, twist, camber or incidence

Wing chord	3.89 feet
Wing span	12.0 feet

Wing Drag

The C_L required for level flight at M_o 3.0 at 50,000 feet is .1305, giving $\alpha = 6.78^o$ and $C_D = .0114$ for the proposed design. The closest values that could be found for the biconvex wing were $C_L = .141$, $\alpha = 3.31^o$, and $C_D = .0233$. The scale factor of the model was about 20 and the effect of the change in Reynold's number wasn't considered. In addition, the effects of interference, helical flow about the configuration, and compression and expansion were not considered for the proposed design. The effect of considering a finite wing in the one case and an infinite wing in the other case is minimized since a C_L was selected from infinite wing considerations and the α and C_D merely transcribed for this value. Conservatively, then, the drag of the conventional wing is approximately twice as great as the drag of the proposed design.

Wing Weight

If it is assumed that the spanwise lift distribution and weight per spanwise foot of the two wings are approximately the same, the wings can each be broken at the same spanwise station and the couple loads considered. Taking the couple load to be 190,000 inch pounds, a Q can be found: $190,000 = M = dQC$ where d is the effective couple arm and C is the structural chord. The d of the conventional wing was taken as 1.0 inch and the C, 50% of the local chord (25% to 75% MAC), to be 18.0 inches. This gave a Q of 10550 pounds per inch. For the proposed design, d was taken as 5.18 inches and C, 73% of the local chord (27% to 100% MAC for reasons previously discussed), to give a Q of 1080 pounds per inch.

Table 4 of ref. 10 gives the required cross-section area for the upper wing

surface as 6.6296 square inches for the conventional wing. If, for the proposed design, it is assumed that the shock generator and burner wall carry no load and are equal in weight to the skin and stringers, this will give a load carrying cross section of 3.33 square inches for a wing of the same weight per lineal foot. This gives a Q of about 3,000. Therefore, the proposed design of engine and wing the same weight as the conventional wing alone has about 2.78 times the maneuver load capability of the conventional wing.

No mention has been made of the weight of the engine and nacelle attached to the conventional wing, the wave drag and skin friction drag of the nacelle, and the interference of the nacelle and wing. Thus it can be seen that the proposed configuration is lighter by the weight of the engine and nacelle, is over 2.5 times as strong, provides no interference, and has much less drag (approximately one-half the wing drag with no drag corresponding to the nacelle drag of the conventional configuration). The reduction in wing weight and interference provides an additional reduction in drag, which taken with the previous drag reduction would greatly increase the range for a given amount of fuel, reduce the power required, and still maintain the 2.5 strength ratio over the conventional wing.

CONCLUSIONS

From the foregoing it can be concluded that:

1. The proposed configuration is theoretically feasible.

2. A unique diffuser configuration can be obtained for any desired cruise speed.

3. This diffuser configuration offers high total pressure recovery over a wide range of supersonic flight speeds, and superior design point operation.

4. A constant diffuser throat area and Mach number can be maintained during operation over a wide range of flight Mach numbers.

5. A constant burner inlet Mach number can be maintained during operation over a wide range of flight Mach numbers.

6. The constant throat area and Mach number and burner inlet Mach number permit an optimum performance subsonic diffuser.

7. The variable exit nozzle proposed offers improved thrust over a wide range of flight speeds and altitudes.

8. The two dimensional flow considered permits engine and intake geometry to be varied by simple mechanical means.

9. The integration of a ramjet power plant with a ducted lifting surface offers the following significant performance gains in the supersonic flight regime:

(a) Greatly reduced drag

(b) Stronger construction

(c) Less weight

10. The ramjet engine that has been proposed provides sufficient thrust to propel the vehicle considered for operation over a wide range of supersonic Mach

numbers and altitudes.

11. The integrated system has practically constant orientation to the relative wind; so the variable geometry of the diffuser can be made solely a function of flight Mach number.

12. These variable diffuser surfaces are in part balanced by air loads; so that the structural requirements are not great, and the power required to position the surfaces is reasonable.

13. Aeroelastic effects are greatly reduced to provide design simplification.

14. There are a minimum number of moving parts, and none move rapidly enough to build up dynamic loads.

15. These moving parts have counterparts on normal aircraft, and can be controlled by single common sensing devices.

16. It has been shown theoretically that the configuration is highly maneuverable over a wide range of flight speeds, this from the high thrust to drag ratio as well as the increased structural strength and lift capability.

17. Due to the greatly reduced weight and drag, and thus thrust requirements; a smaller vehicle can be built that is capable of the same range and payload.

18. The design can be broken down into three areas; the supersonic diffuser, the engine, and the wing. These three areas are no more difficult, and in most cases simpler, to design and manufacture than their normal counterparts.

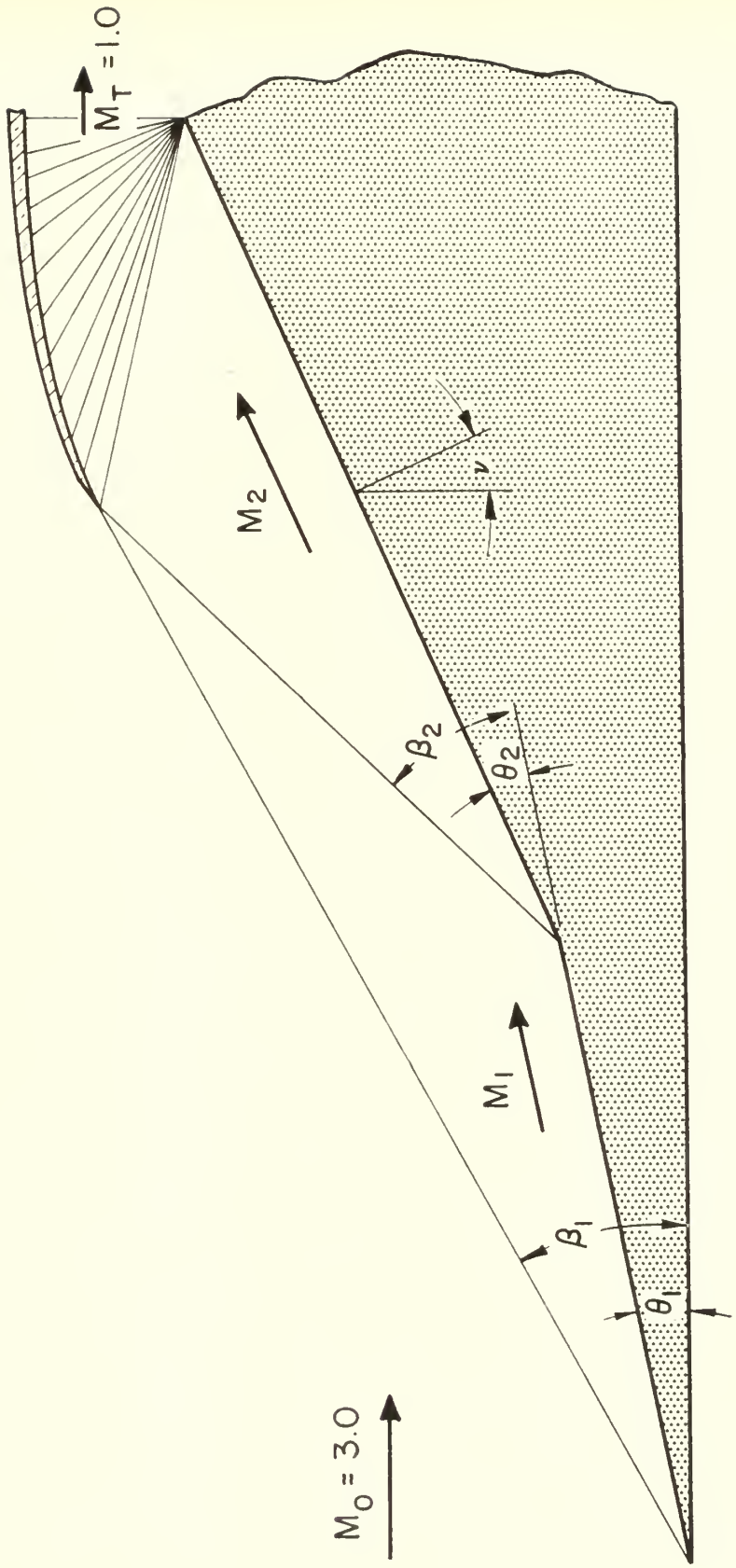

Fig. 1.

Optimum Configuration for $M_{DP} = 3.0$

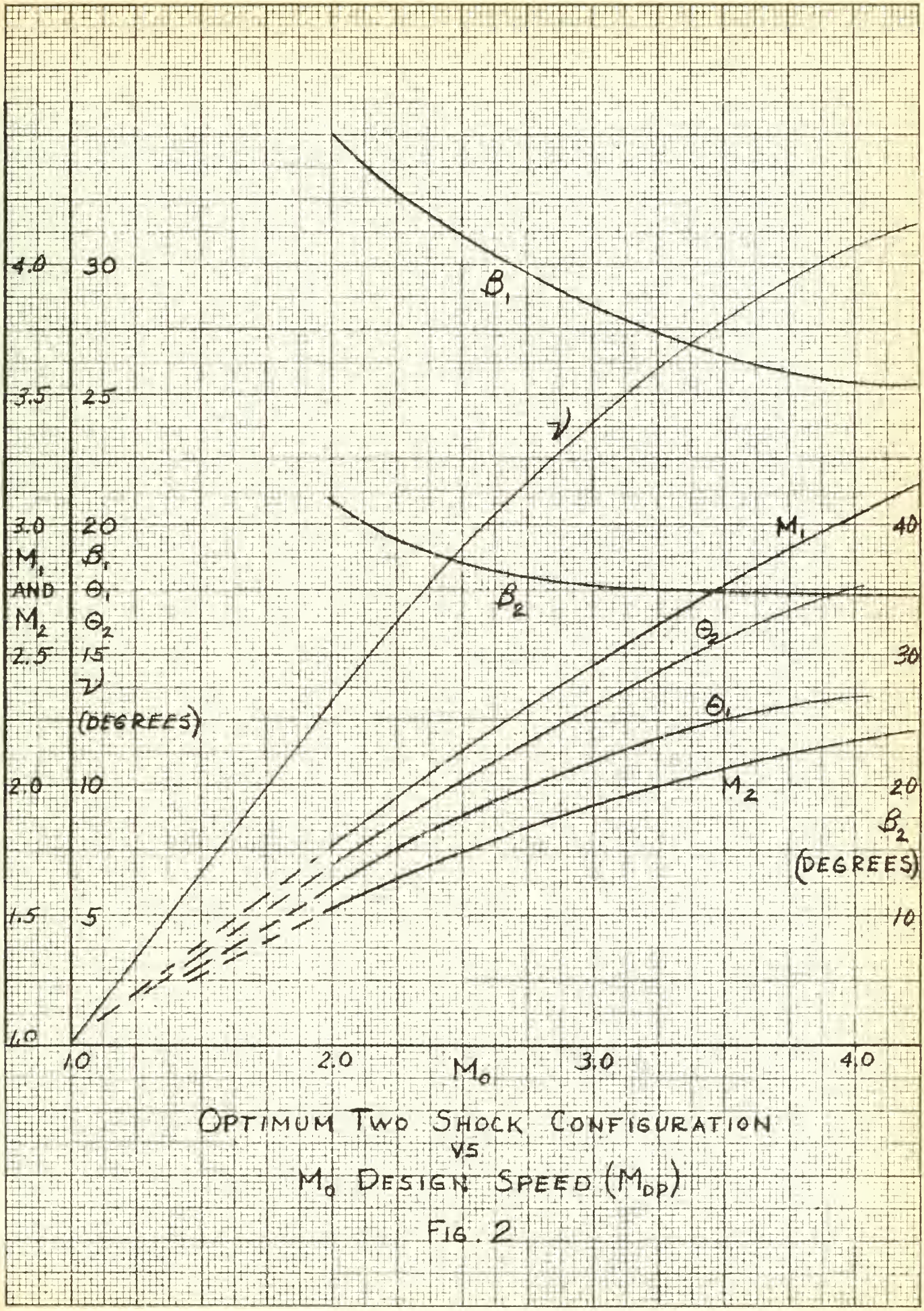

OPTIMUM TWO SHOCK CONFIGURATION
VS
M_o DESIGN SPEED (M_{DP})

FIG. 2

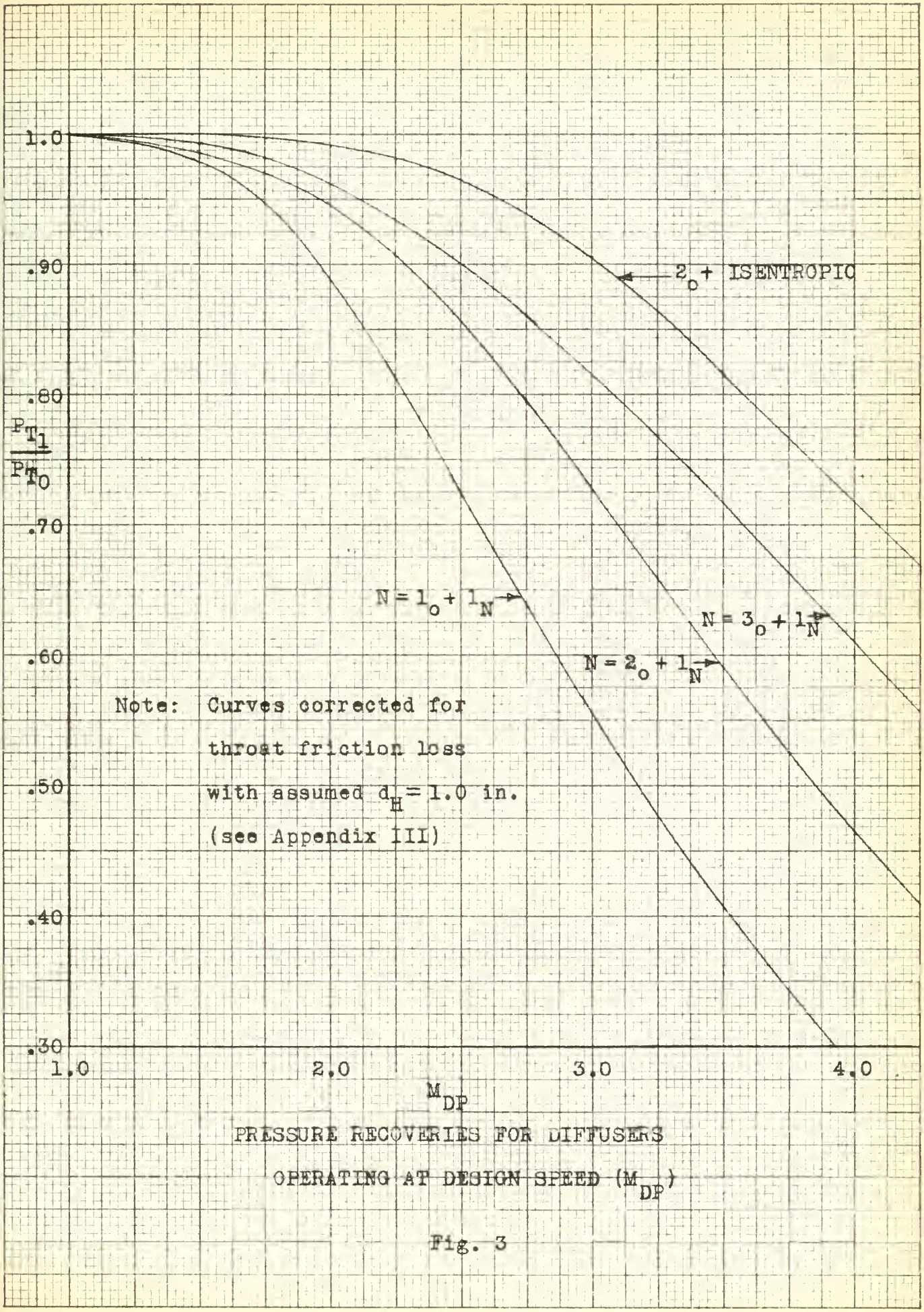

PRESSURE RECOVERIES FOR DIFFUSERS OPERATING AT DESIGN SPEED (M_{DP})

Fig. 3

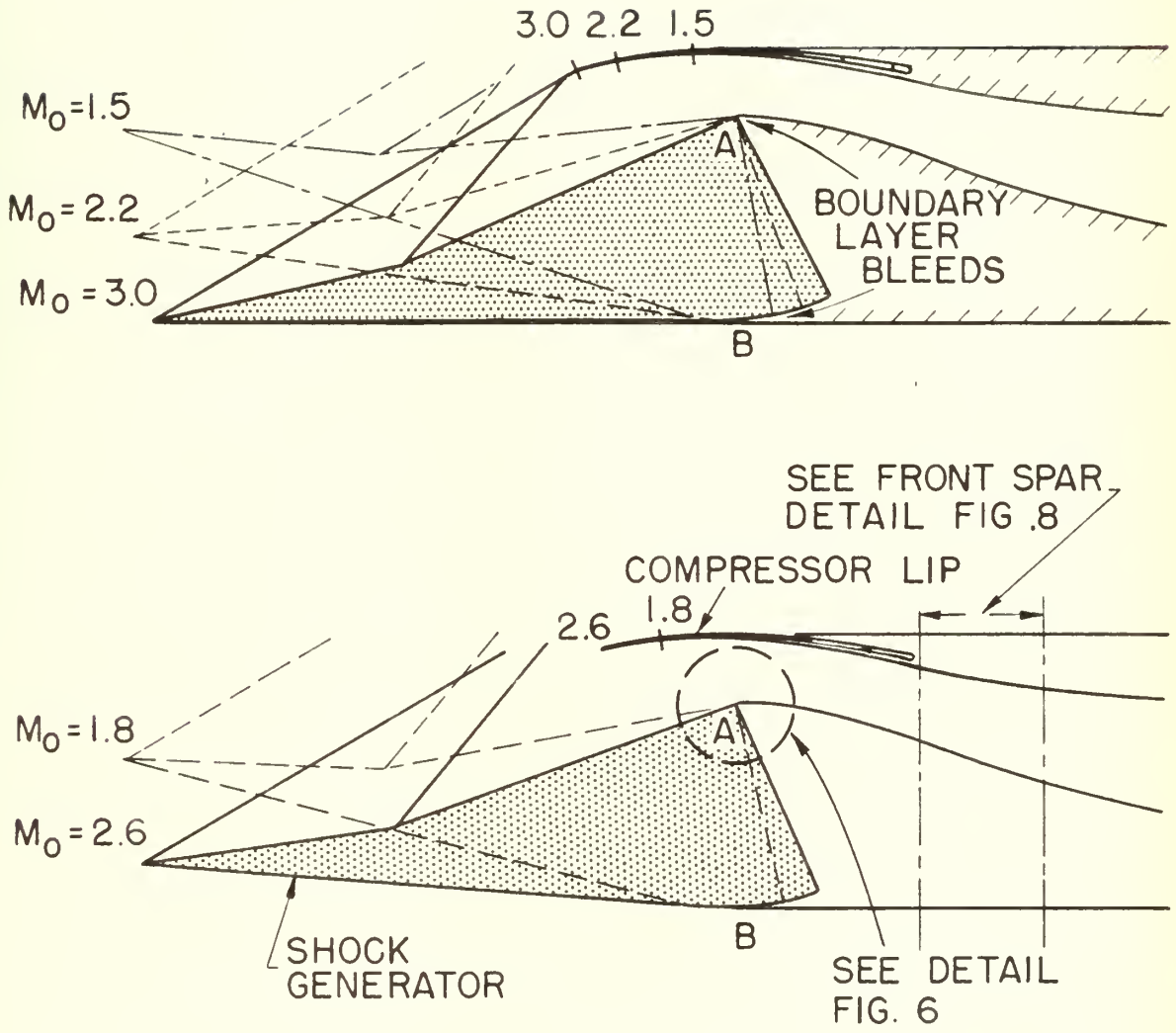

Fig. 4.

Schematic – Two Shock System

Shock Generator and Compressor Lip Position

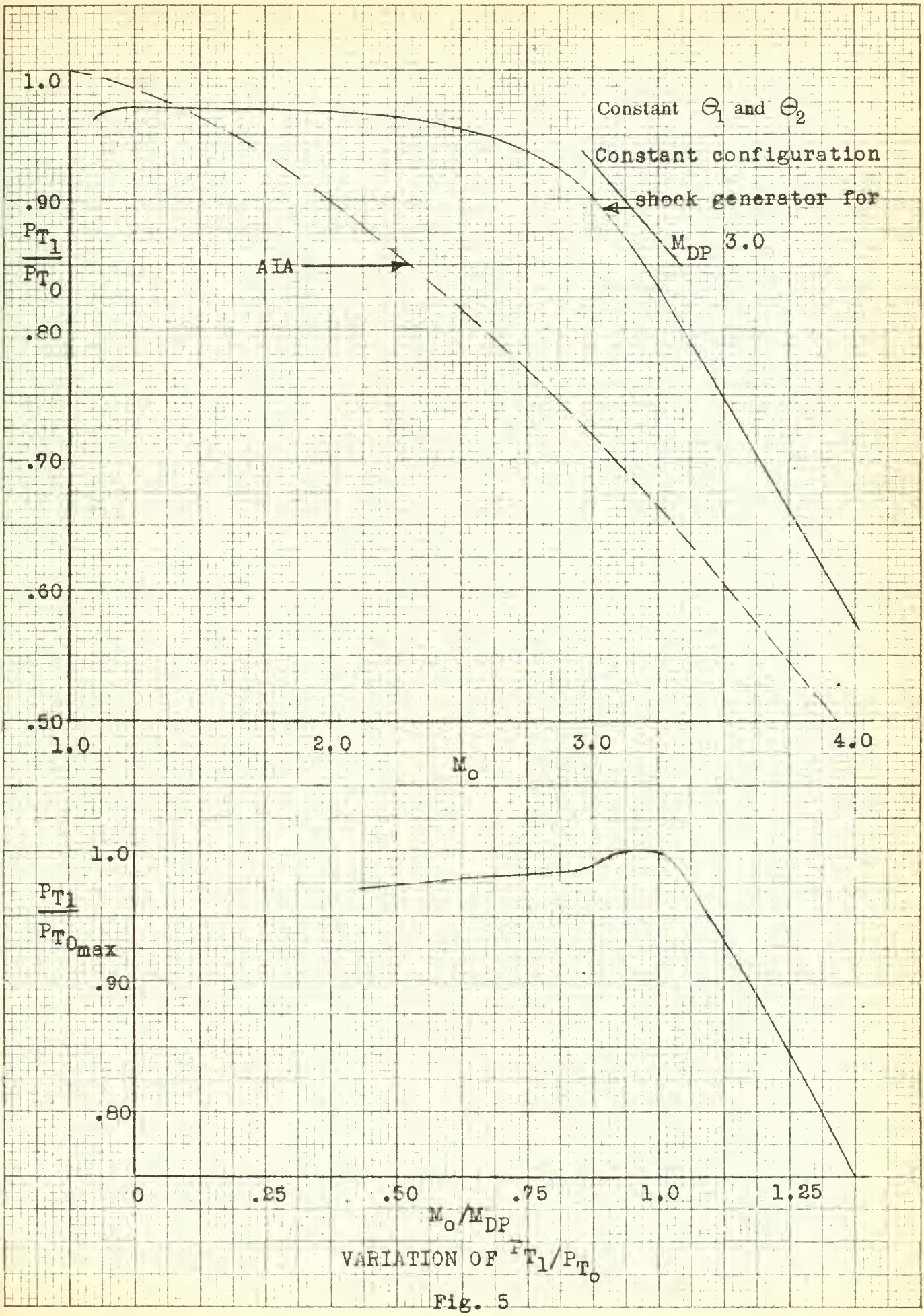

VARIATION OF P_{T_1}/P_{T_o}

Fig. 5

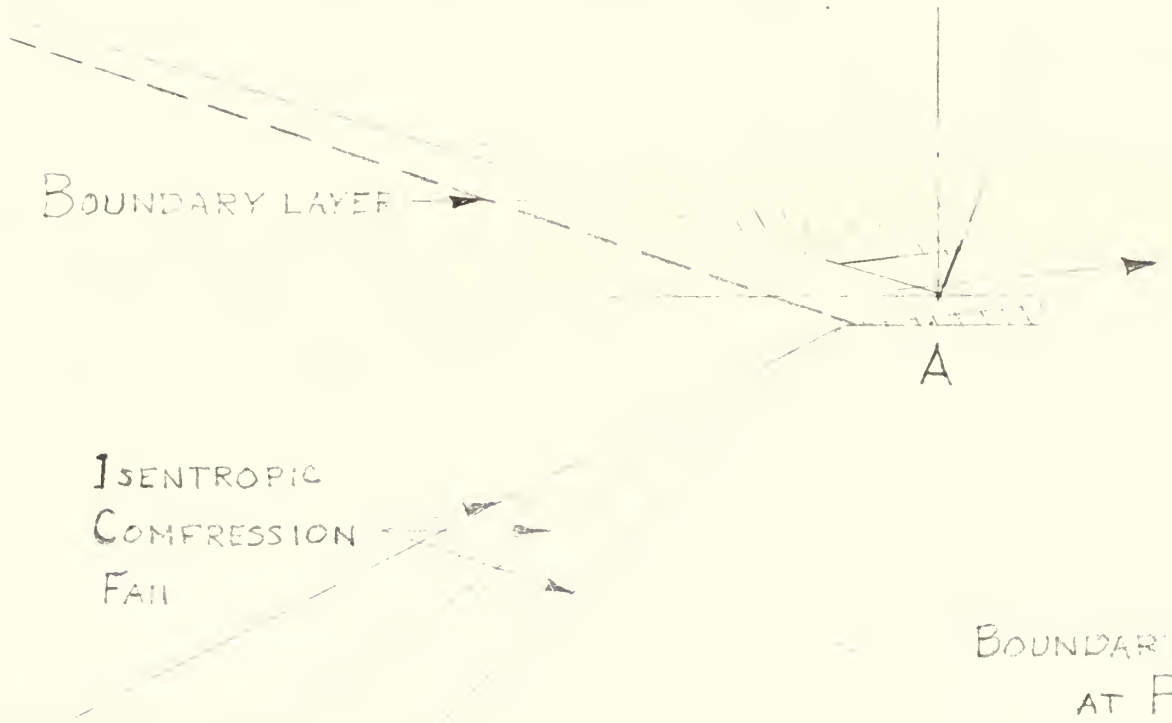

BOUNDARY LAYER BLEED
AT POINT A
FIG. 6

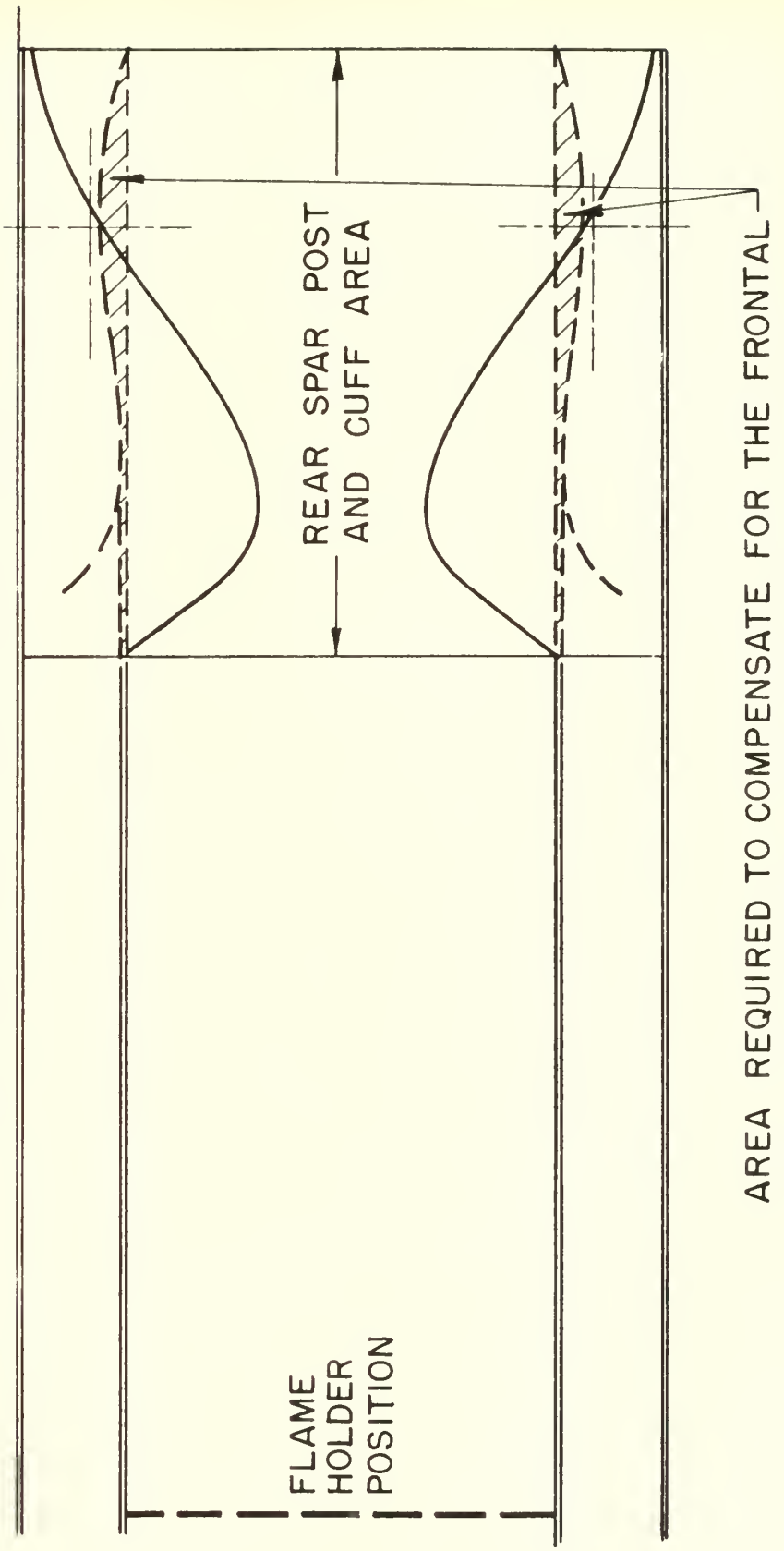

Fig. 7.
Wing Cross Section Rear Spar Area Detail

Fig. 8

Wing Cross Section at a Front Spar Post Detail

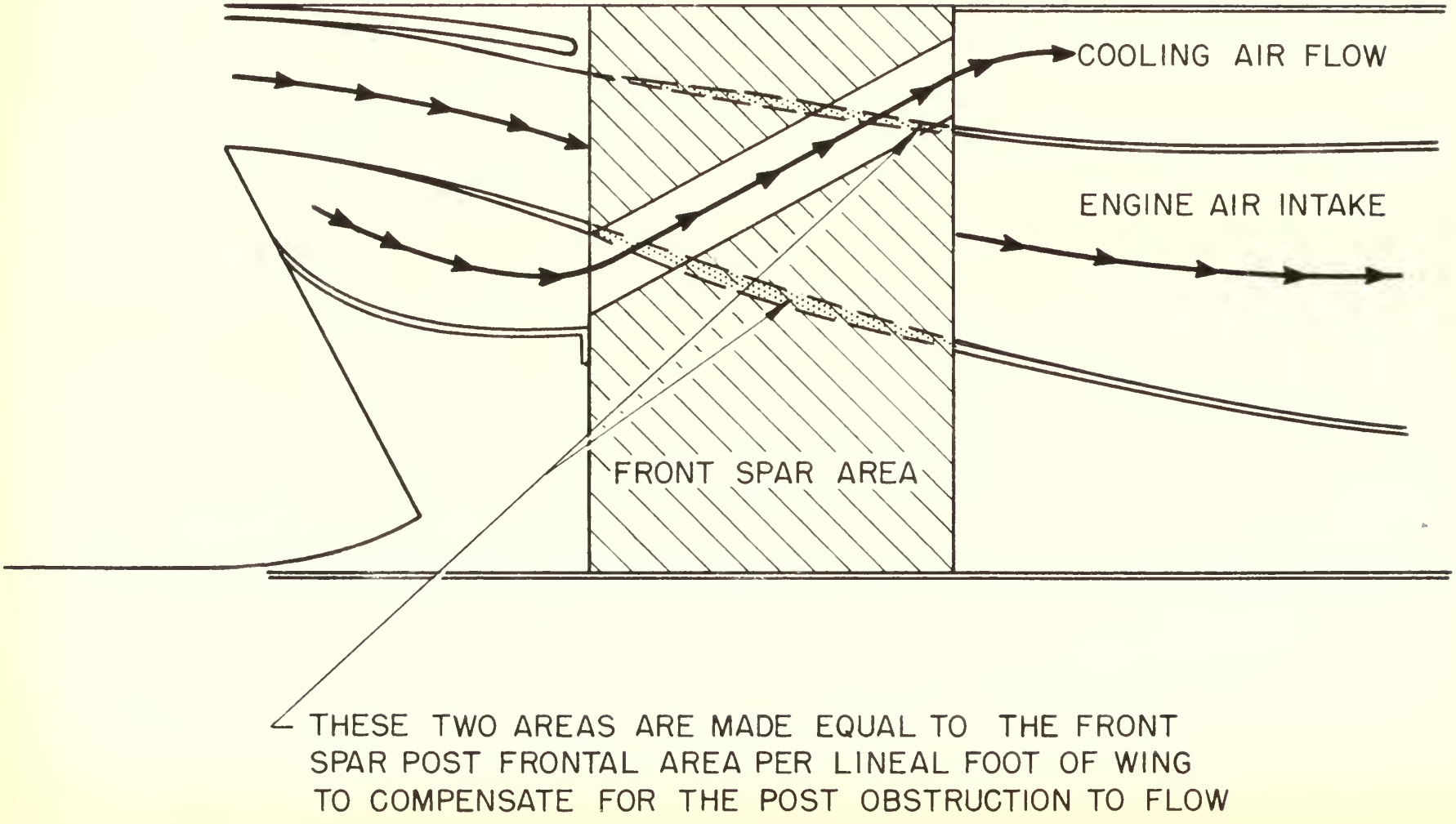

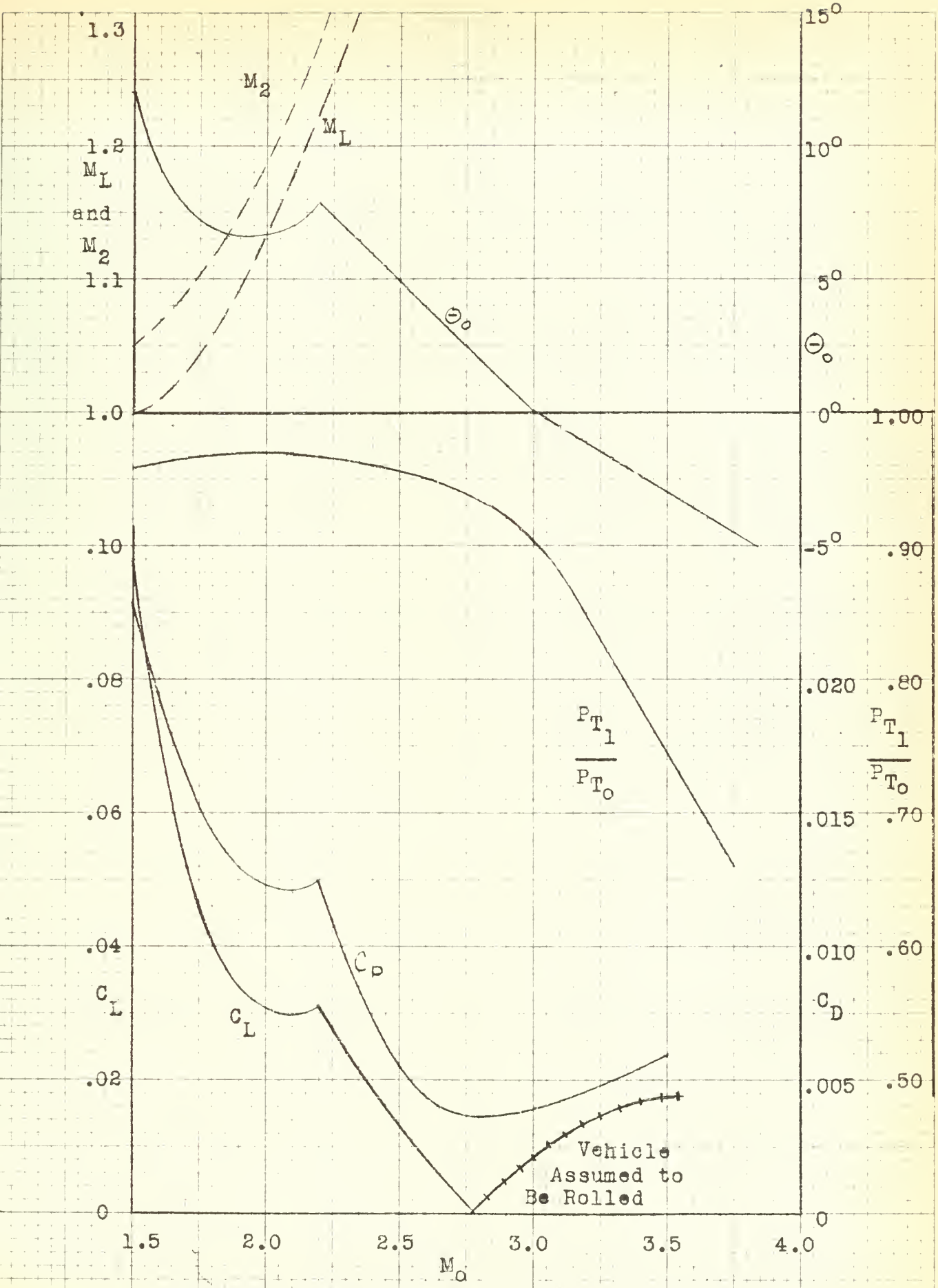

DIFFUSER OPERATION PER LINEAL FOOT OF WING

Fig. 9

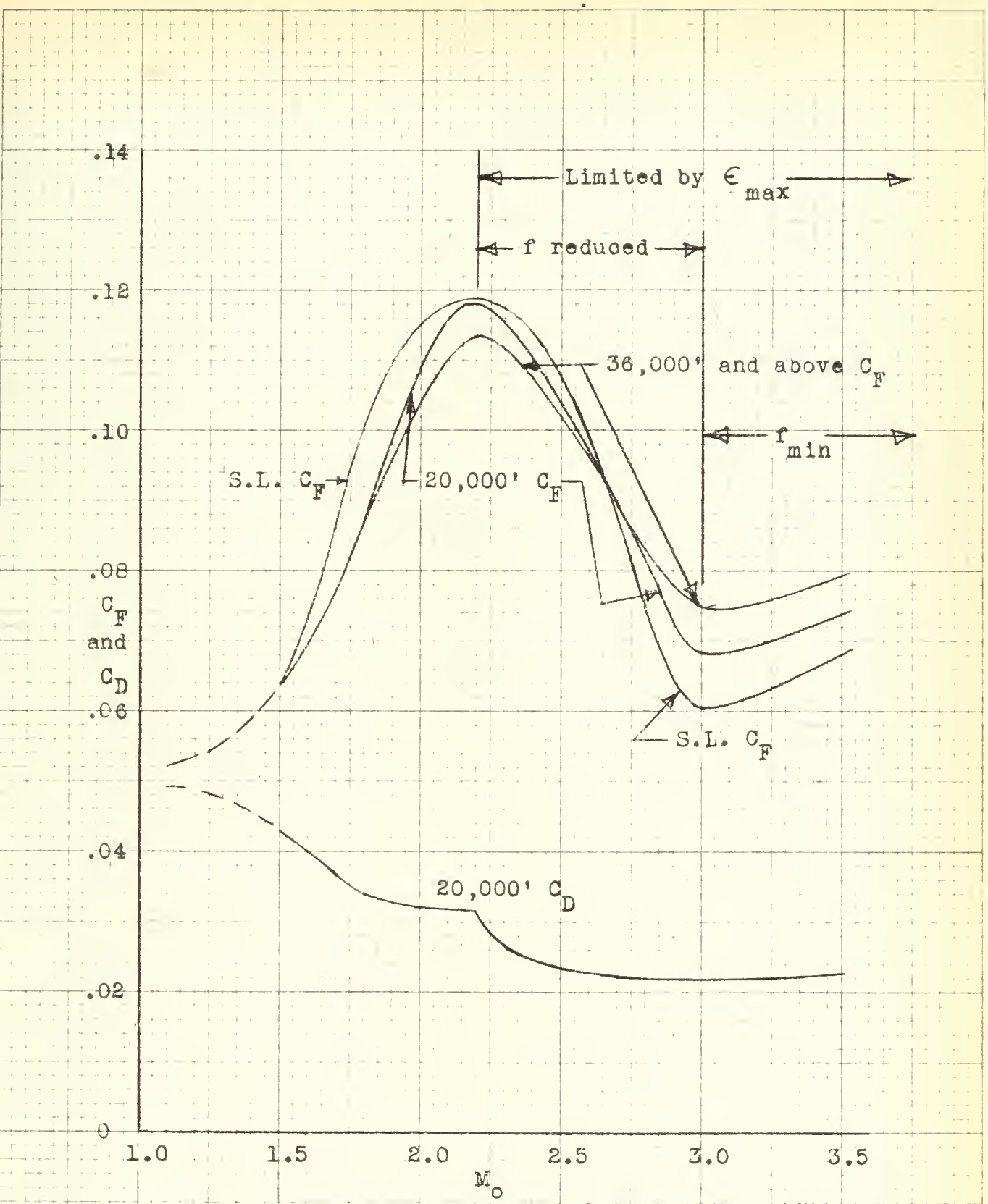

TOTAL C_D AND C_F VERSUS M_o

Fig. 10

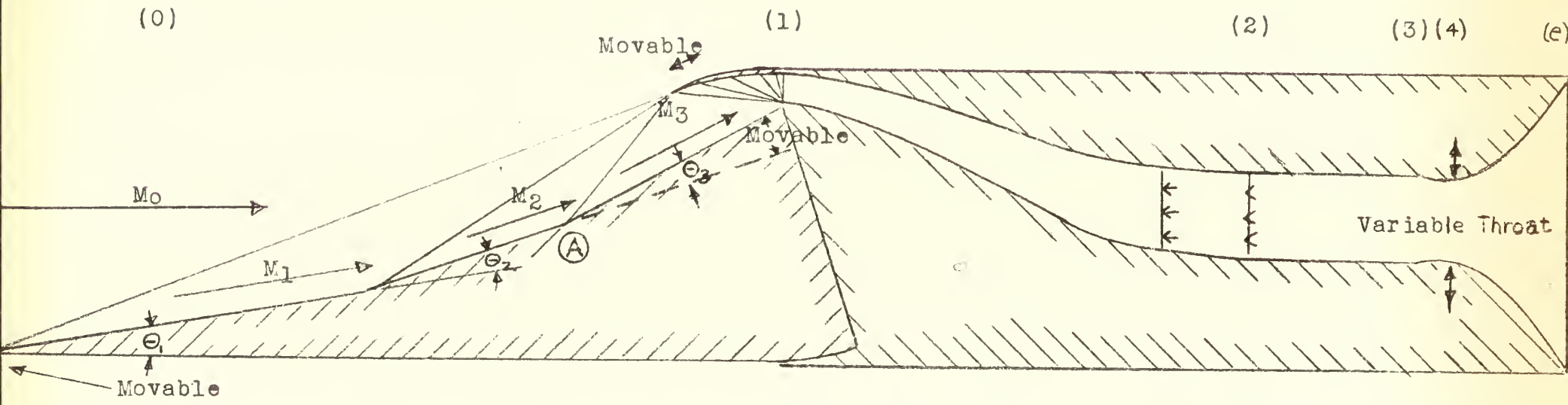

Note: The third ramp is hinged at Point A and can be lowered to make $\Theta_3 = 0^\circ$

SCHEMATIC - THREE SHOCK SYSTEM WITH M_{DP} 4.0

Fig. 11

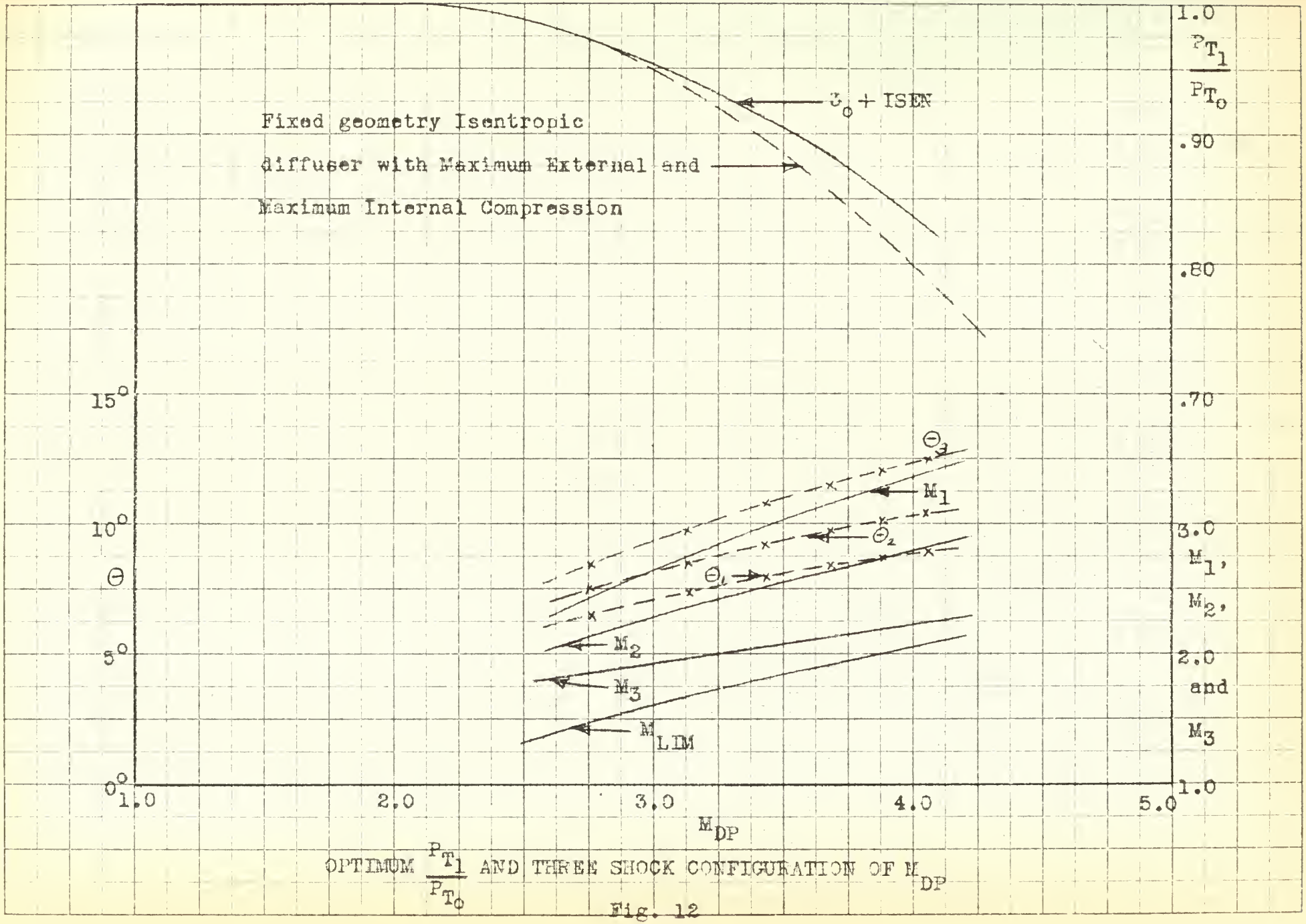

OPTIMUM $\frac{P_{T_1}}{P_{T_0}}$ AND THREE SHOCK CONFIGURATION OF M_{DP}

Fig. 12

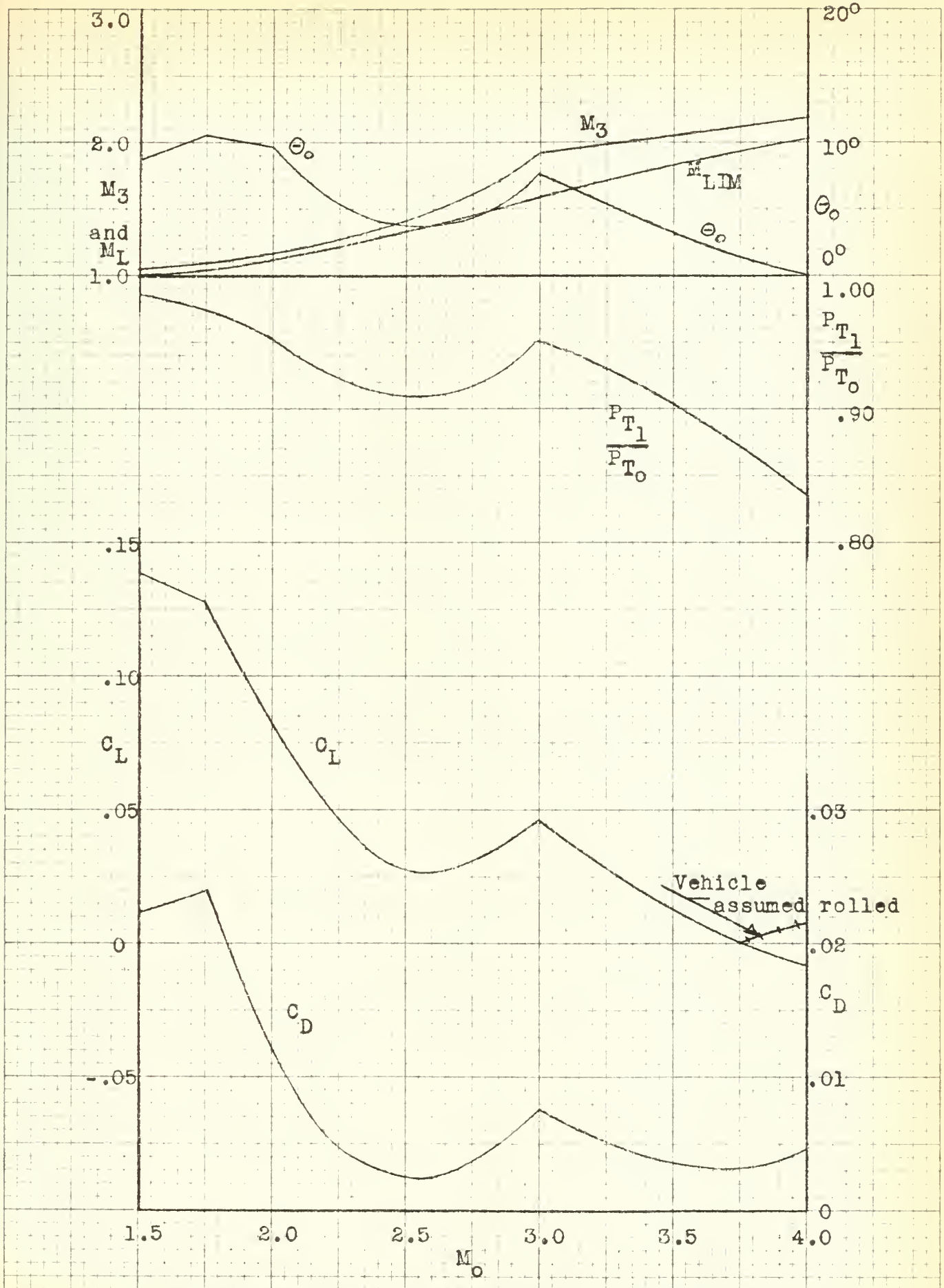

DIFFUSER OPERATION PER LINEAL FOOT OF WING

Fig. 13

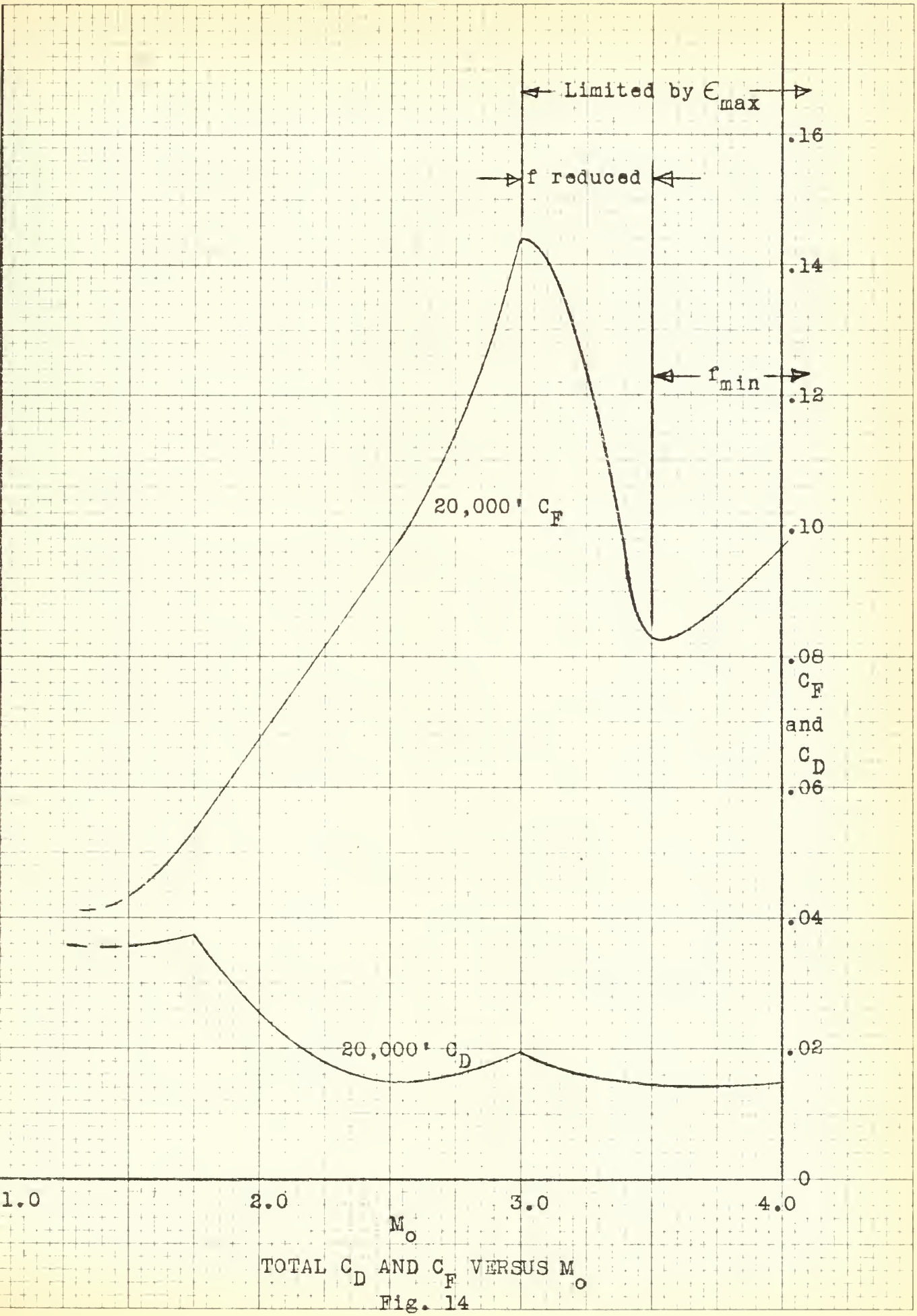

TOTAL C_D AND C_F VERSUS M_o

Fig. 14

REFERENCES

1. Nicholson, L. F. "Engine-Airframe Integration" Journal of the Royal Aeronautical Society; Nov. 1957

2. Oswatitsch, K. English Translation: "Pressure Recovery for Missiles with Reaction Propulsion at High Supersonic Speeds (The Efficiency of Shock Diffusers)" NACA TM 1140; June 1947

3. Kuethe, A. M. and Schetzer, J. D. "Foundations of Aerodynamics" John Wiley and Sons, New York, N. Y.; 1950

4. Connors, J. F. and Meyer, R. C. "Design Criteria for Axisymmetric and Two-Dimensional Supersonic Inlets and Exits" NACA TN 3589; Jan. 1956

5. Dailey, C. L. and Wood, F. C. "Computation Curves for Compressible Fluid Problems" John Wiley and Sons, New York, N. Y.; 1949

6. Hermann, R. "Supersonic Inlet Diffusers and Introduction to Internal Aerodynamics" Minneapolis-Honeywell Regulator Co., Minneapolis, Minn.; 1956

7. Sutton, G. P. "Rocket Propulsion Elements" John Wiley and Sons, New York, N. Y.; 1956

8. Bonney, E. A., Zucrow, M. J., and Besserer, C. W. "Aerodynamics, Propulsion, Structures and Design Practice" D. Van Nostrand Co., Inc. Princeton, N. J.

9. Donovan, A. F. and Lawrence, H. R. (editors) "Aerodynamic Components of Aircraft at High Speeds"; Vol. 7 of "High Speed Aerodynamics and Jet Propulsion"; Princeton University Press; 1957

10. Kolom, A. L. "Optimum Design Considerations for Aircraft Wing Structures"; IAS Paper; Los Angeles, July 1953.

CALCULATION OF PERFORMANCE OF A TWO SHOCK SYSTEM, M_{DP} 3.0

APPENDIX I

The performance of a vehicle using the proposed system was calculated by finding the lift coefficient required for level flight of the vehicle with an assumed wing loading of 200 lb./ft.^{2}; the drag coefficient of the wing when producing the required C_L; the C_D of the rest of the vehicle related to the wing chord per spanwise foot of wing; the inlet momentum term per foot of wing, $\dot{w}\, V_o/g$, related to the wing and expressed in dimensionless coefficient form:

$$C_{F_o} = \frac{\dot{w}\, V_o}{g} \Big/ \frac{\gamma}{2} \quad M_o^2 \, C$$

and the exhaust momentum term per foot of wing:

$$C_{F_e} = \frac{C_f \; P_{T_3} \; A_T}{\gamma/2 \; M_o^2 \; C}$$

For level flight, then:

$$C_{F_e} - C_{F_o} = C_F = C_{D_{Body}} + C_{D_{wing}}$$

since doubling the throat height doubles the wing chord; C_{F_e}, C_{F_o}, and $C_{D_{wing}}$ are independent of throat height for any given configuration with constant wing loading. Therefore, a throat height of one inch and thus the configuration discussed in the text was used for calculation. This made the wing chord equal to three feet.

CALCULATION OF C_F

The station numbers used as subscripts in the following calculations are given in the list of symbols. The following assumptions are made:

Subsonic compressor efficiency, P_{T_2} / P_{T_1}		.90
Burner efficiency		.90
Specific heat of combustion products		1.30
Fuel air ratio:	f_{max}	.071
	f_{min}	.010
Heating value of the fuel	HV	19,000 BTU/lb

No friction losses in the burner

Isentropic flow through the exhaust nozzle

ICAO Standard Atmosphere conditions

Adiabatic flow through the diffuser

The following calculations are made in Table I: The total pressure to static pressure ratio of the free stream flow is given by the formula:

$$P_{T_o}/P_o = \left(1 + \frac{\gamma - 1}{2} M_o^2\right)^{\frac{\gamma}{\gamma - 1}}$$

This ratio is given on Line 1. The ratio at the entrance to the burner will therefore be:

$$P_{T_{2/P_o}} = \left(P_{T_{1/P_{T_o}}}\right)\left(P_{T_{2/P_{T_1}}}\right)\left(P_{T_o/P_o}\right)$$

where $P_{T_{1/P_{T_o}}}$ is given on Fig. 3 as a function of M_o. In the case of M_o 1.5, this ratio was reduced to .959 by the off-optimum diffuser position discussed in the text. $P_{T_{2/P_o}}$ is given on Line 2.

The total temperature ratio of the adiabatic flow, $T_{T_{2/T_o}}$ is given on Line 3, with the total temperature given on Line 4 from the formula:

$$\left(T_{T_o/T_o}\right) T_o = T_{T_2} = T_{T_o}$$

where T_o was taken from ICAO Tables. The increase in total temperature through the combustor is the product of the combustor efficiency and the theoretical temperature rise. This theoretical rise is a function of the inlet total temperature and the fuel-air ratio. In the cases underlined in Lines 5 and 6, this fuel-air ratio (maximum) was more than enough to accelerate the outlet air to M_3 1.0; so for these cases f was reduced to a value that just gave M_3 1.0 (at the exit of the burner). This total temperature rise is given on Line 5 with the burner outlet total temperature (Line 4 plus Line 5) given on Line 6.

For the addition of heat in a constant area duct in the absence of friction it is possible to obtain a relation between the total temperature ratio and the Mach number from a ϕ function or Rayleigh Line Chart. For a constant burner inlet Mach number the ϕ function will be constant and was found to be .0367. $\phi(M_3)$ can then be found from the relation:

$$\phi(M_3) = \phi(M_2) \; {}^{T}T_{3/T_{T_2}} \quad \text{or .0367 X Line 7}$$

$\phi(M_3)$ can then be used to re-enter the chart to find the burner exit Mach number. The values found for the exit are given on Line 9. ${}^{T}T_{3/T_{T_2}}$ is given on Line 7, and $\phi(M_3)$ values are given on Line 8.

With an assumed height of the diffuser throat of one inch, the height of the burner for a constant M_2 is constant and given by the A/A* ratio for γ of 1.4. The burner height was found to be 2.965 inches. Writing the continuity equation at the exit nozzle throat and the diffuser gives the ratio:

$$\frac{A_{N_T}}{A_{D_T}} = \frac{M_{DT}}{M_{NT}} \; \frac{P_T)_{DT}}{P_T)_{NT}} \left[\frac{T_T)_{NT}}{T_T)_{DT}}\right]^{1/2} \left[\frac{1+\frac{\gamma-1}{2} M^2_{NT}}{1+\frac{\gamma-1}{2} M^2_{DT}}\right]^{\frac{\gamma+1}{2(\gamma-1)}}$$

Since both throats are choked, this simplifies to:

$$\frac{A_{N_T}}{A_{D_T}} = \frac{\sqrt{\gamma/R)_{DT}}}{\sqrt{\gamma/R)_{NT}}} \left\{ P_{T_1/P_{T_2}} \right\} \left(P_{T_2/P_{T_3}} \right) \left(T_{T_3/T_{T_2}} \right)^{1/2}$$

The first ratio was found to be .96; and the second ratio was assumed to be 1/.90.

$P_{T_2/P_{T_3}}$ was found from the formula:

$$\frac{P_{T_2}}{P_{T_3}} = \frac{P_{T_2/P_2}}{1 + \gamma M_2^2} \qquad \frac{P_{T_2/P_3}}{1 + \gamma M_3^2}$$

For constant M_2, the first ratio is a constant and was found to be .9735. The second ratio was found from a chart[5] for a γ of 1.3. These values are shown on Line 10. Therefore:

$$P_{T_{2/P_{T_3}}} = .9735/\text{Line } 10$$

This is shown on Line 11. If one lineal foot of wing is considered:

$$12\ A_{NT} = 1.158 \times \text{Line } 11 \times (\text{Line } 7)^{1/2}$$

These values are shown on Line 12. P_{T_3/P_o} was obtained by dividing Line 2 by Line 11. These values are shown on Line 13. This value was then used to enter Thrust Coefficient vs. Area Ratio Tables to get C_f and ϵ for optimum expansion. The results are given on Lines 14 and 15. The area of the exit was then calculated using:

$$A_e = A_T \epsilon \qquad \text{or} \qquad \text{Line } 12 \times \text{Line } 15$$

The results are given on Line 16. In cases where the optimum exit area was limited by the thickness of the wing (those values starred), it was assumed that f was reduced to reduce the Mach number at the exit of the burner and thus reduce A_T to the optimum value of ϵ for $C_{f_{max}}$. These reduced values are shown on Line 12.5. In order to simplify calculations it was assumed that λ,

the correction factor for the divergence angle of the exhaust nozzle was unity; and that even though f was reduced greatly, the total pressure and total temperature loss remained the same. It was felt that this was very conservative. In the range M_o 3.0 and greater this f value required for optimum ϵ got below the assumed minimum fuel flow. Values for f of .010 were therefore recalculated in the short table after Line 16, and are shown in the table starting with Line 17. The values of C_f found for this condition are shown in the table. It should be noted that they range from 99.6% to 97.7% of the previous optimum C_f.

The exhaust thrust divided by the static pressure was found from:

$$\frac{F_e}{P_o} = \frac{C_f \ 12 \ A_T}{12} \left(\frac{P_{T_3}}{P_o}\right) \quad \text{or} \quad \frac{\text{Line 12 X Line 13 X Line 14}}{12}$$

The results are given on Line 17. This was converted to C_{F_e} on Line 18.

C_{F_o} was computed from the equation:

$$C_{F_o} = \frac{\dot{w} \, V_o}{g} \Big/ \frac{\gamma}{2} \ P_o \, M_o^2 \, C$$

$\dot{w}$ was found by finding a constant:

$$\frac{\dot{w}\sqrt{\theta_{t_2}}}{A_2 \, \delta_{t_2}} = \frac{P_o}{\sqrt{T_o}} \ M_2 \left(1 + \frac{\gamma - 1}{2} M_2^2\right)^{-\frac{\gamma+1}{2(\gamma-1)}} \sqrt{\frac{\gamma \, g}{R}} = 16.75$$

where: $\theta_{t_2} = (T_{T_2/T_o})(T_{alt}/T_{S.L.})$

$$\delta_{t_2} = (P_{T_2/P_o})(P_{alt}/P_{S.L.})$$

Values of δ_{t_2} are given on Line 19, values of $\sqrt{\theta_{t_2}}$ are given on Line 20; and values of $\dot{w}$ are given on Line 21. C_{F_o} will be the same at all altitudes; so only the values of V_o/g for sea level are given on Line 22. C_{F_o} values are given on Line 23. The engine coefficient of thrust is therefore:

$$C_F = C_{F_e} - C_{F_o} \quad \text{or Line 18 - Line 23.}$$

This is shown on Line 24 and in Fig. 10.

CALCULATION OF C_L AND C_D

The C_L required for level flight was found by the formula:

$$C_L = \frac{W/S}{\gamma/2 \; P_o \; M_o^2} \qquad \text{where } W/S = 200 \text{ lb./ft.}^2$$

These values are shown on Line 25.

Showing the thrust to be well over the drag for one altitude demonstrates the ability of the vehicle to accelerate to cruise speed. Using a throat height of two inches makes all the cross-section dimensions twice as big as those discussed in the text. This makes the actual chord:

1.625 ft. (generator) + 4.375 ft. (aft wing) = 6 ft.

generator chord = .271 total chord

aft wing chord = .729 total chord

The height of the throat is limited by the length of generator that can be controlled and held in place; but 1.625 ft. seemed very reasonable. The C_L and C_D of the shock generator were computed from values of Θ_o given on Fig. 9, using Linearized Thin Airfoil Theory. The results are given on Fig. 9 and in Lines 26 through 30. The body shape discussed in the text with R_{max} of 1.38 ft. was assumed. The C_D values related to the wing chord are given on Line 31, with the total C_D given on Line 32, and in Fig. 10. Lines 26 through 30 assumed that the vehicle could be rolled 180^o (turned upside-down) for cruise in order to keep the angle of attack nearly constant at zero degrees. The short table following Line 32 was used to investigate the effect of rolling the vehicle at M_o 3.0 and greater speeds. It can be seen in both cases that C_F is well above C_D.

In order to simplify calculations, the lift of the body and tail surfaces, and the relatively large portion of the wing submerged in the fuselage were ignored. This would be offset somewhat by the non-linear effects of interference of wing and wing, and wing and body that were also ignored; but the simplification will still be conservative. The calculations were further simplified by making a pessimistic estimate of the lumped drag effects of body, tail, and submerged wing.

TABLE I-1

CALCULATION OF PERFORMANCE OF A TWO SHOCK SYSTEM, M_{DP} 3.0

M_o	1.5	1.75	2.2	2.6	3.0	3.5	4.0	Alt.	Line
P_{T_o}/P_o	3.67	5.33	10.7	19.95	36.7	76.2	152	-	1
P_{T_2}/P_o	3.2	4.65	9.3	17.01	29.9	51.2	78.4	-	2
T_{T_2}/T_o	1.45	1.612	1.97	2.35	2.80	3.45	4.20	-	3
T_{T_2}/T_o	751	836	1022	1219	1452	1790	2180	OK	4
	648	721	881	1052	1252	1543	1879	20K	
	565	629	768	916	1092	1346	1639	36K	
T_T added	2559	3065	3000	2946	2870	2760	2640	OK	5
	2207	2559	3050	2995	2930	2835	2730	20K	
	1925	2141	2612	3035	2980	2895	2802	36K	
T_{T_3}	3310	3901	4019	4165	4322	4550	4820	O K	6
	2835	3180	3928	4047	4182	4378	4609	20K	
	2490	2770	3380	3959	4072	4241	4441	36K	
T_{T_3}/T_{T_2}	4.41	4.66	3.95	3.42	2.98	2.54	2.22	O K	7
	4.41	4.41	4.46	3.845	3.34	2.835	2.455	20K	
	4.41	4.41	4.41	4.33	3.73	3.15	2.70	36K	
$\phi(M_3)$	.2172	.171	.145	.1265	.1092	.0931	.0814	O K	8
	.2172	.2172	.1637	.141	.1225	.1040	.090	20K	
	.2172	.2172	.2172	.1589	.1369	.1156	.0990	36K	
M_3	.65	.58	.49	.438	.392	.351	.321	O K	9
	.87	.688	.553	.48	.427	.378	.343	20K	
	1.00	1.00	.636	.536	.466	.408	.366	36K	

M_o	1.5	1.75	2.2	2.6	3.0	3.5	4.0	Alt.	Line
$\frac{P_{T_3}/P_3}{1+\gamma M_3^2}$	.797	.861	.888	.905	.920	.933		0 K	
	.797	.797	.869	.892	.909	.924	γ=1.3	20K	10
	.797	.797	.797	.874	.896	.915		36K	
P_{T_2}/P_{T_3}	1.22	1.13	1.095	1.075	1.059	1.042		0 K	
	1.22	1.22	1.12	1.09	1.071	1.052		20K	11
$= \frac{.9735}{(10)}$	1.22	1.22	1.22	1.111	1.086	1.062		36K	
12 A_{NT}=	2.965*	2.825	2.52	2.30	2.116	1.925		0 K	
	2.965*	2.965*	2.74	2.47	2.24	2.047		20K	12
1.158 (11)(7)	2.965*	2.965*	2.965*	2.68	2.437	2.185		36K	
12 A_{NT}			2.10	1.60				0 K	
			2.16	1.611				20K	12.5
(corrected)			2.22	1.64				36K	
P_{T_3}/P_o	2.622	4.11	8.49	15.82	28.22	49.2		0 K	
	2.622	3.81	8.3	15.6	27.9	48.75		20K	13
$= \frac{(2)}{(11)}$	2.622	3.81	7.62	15.3	27.55	48.25		36K	
	.875	1.04	1.23*	1.332*	1.45	1.515		o K	
C_f	.875	1.02	1.22*	1.33*	1.448	1.513		20K	14
	.875	1.02	1.208*	1.325*	1.445	1.511		36K	
	1.03	1.29	1.9*	2.5*	4.2	5.9		0 K	
ϵ	1.03	1.25	1.85*	2.48*	4.17	5.88		20K	15
	1.03	1.25	1.8*	2.44*	4.15	5.85		36K	
	3.05	3.82	4.0	4.0	4.0	4.0		0 K	
A_e	3.05	3.705	4.0	4.0	4.0	4.0		20K	16
	3.05	3.705	4.0	4.0	4.0	4.0		36K	

SHORT TABLE I-2

o K		20K		36K		Alt.
3.0	3.5	3.0	3.5	3.0	3.5	M_o
1992	2330	1792	2083	1639	1893	T_{T_3}
1.322	1.301	1.43	1.35	1.49	1.40	T_{T_3}/T_{T_2}
.0486	.0478	.0524	.0495	.0546	.0514	$\phi(M_3)$
.235	.233	.246	.2385	.251	.243	M_3
.967	.9672	.964	.966	.962	.9642	$\frac{P_{T_2}}{P_3}/1+\gamma M_3^2$
1.007	1.006	1.01	1.008	1.011	1.009	P_{T_2}/P_{T_3}
1.34	1.328	1.4	1.354	1.43	1.382	12 A_{NT}
29.7	50.9	29.6	50.8	29.55	50,75	P_{T_3}/P_o
2.985	3.01	2.86	2.95	2.8	2.89	ϵ
1.443	1.463	1.441	1.48	1.439	1.476	C_f
4.79	8.35	4.93	8.48	5.07	8.62	F_e/P_o
.2535	.3245	.261	.330	.286	.335	C_{F_e}

M_o	1.5	1.75	2.2	2.6	3.0	3.5	Alt.	Line
F_e/P_o	.567	1.05	2.195	3.375	see	above	o K	17
	.567	.960	2.190	3.34	see	above	20K	
	.567	.960	2.045	3.32	see	above	36K	
C_{F_e}	.120	.1635	.216	.237	see	above	0 K	18
	.120	.1495	.2155	.235	see	above	20K	
	.120	.1495	.211	.2335	see	above	36K	
δ_{x_2}	3.2	4.65	9.3	17.01	29.9	51.2	o K	19
	1.47	2.135	4.27	7.81	13.62	23.5	20K	
	.719	1.042	2.065	3.82	6.72	11.47	36K	
	.368	.535	1.068	1.955	3.438	5.88	50K	

M_o	1.5	1.75	2.2	2.6	3.0	3.5	Alt.	Line
$\sqrt{\theta_{x_2}}$	1.207	1.27	1.402	1.553	1.672	1.858	OK	20
	1.119	1.179	1.304	1.425	1.555	1.725	20K	
	1.048	1.105	1.221	1.335	1.458	1.616	36K	
$\mathring{w}$	11.0	15.18	27.45	45.9	74.0	114.2	0 K	21
	5.44	7.50	13.65	22.70	36.3	56.4	20K	
	2.84	3.905	7.00	11.85	19.09	29.35	36K	
	1.452	1.965	3.62	6.14	9.75	15.07	50K	
V_o/g	51.9	60.6	76.1	90	103.9	121.7	0 K	22
C_{F_o}	.0571	.0676	.0972	.1373	.1925	.2560	-	23
C_F	.0629	.0959	.1188	.0997	.0610	.0685	0 K	24
	.0629	.0819	.1183	.0977	.0685	.0740	20K	
	.0629	.0819	.1138	.0962	.0755	.0790	36K	
	.0629	.0819	.1138	.0962	.0755	.0790	50K	
C_L	.060	.0439	.02785	.01995	.01494	.01102	0 K	25
	.1305	.0961	.0606	.0435	.03262	.0240	20K	
	.2685	.1968	.1247	.089	.0669	.0491	36K	
	.523	.3835	.243	.1735	.1305	.0960	50K	
$C_{L_{gen.}}$	.0975	.0461	.0305	.00595	.00845	.01733	20K	26
$C_{L_{aft\ wing}}$	.0330	.05	.0303	.03755	.02417	.00667	20K	27
α aft wing	.727°	1.41°	1.17°	1.775°	1.34°	0.44°	20K	28
$C_{D_{aft\ wing}}$	.0002	.0006	.00031	.00058	.00028	0	20K	29
$C_{D_{body}}$	.0202	.0197	.0190	.0182	.0175	.0165	20K	30
$C_{D_{gen}}$	.0227	.0153	.01245	.0039	.0039	.00575	20K	31
$C_{D_{tot}}$	.0431	.0357	.03176	.0227	.0217	.02225	20K	32

SHORT TABLE I-3

M_o 3.0								
	ROLLED				UNROLLED			
Alt.	0	20K	36K	50K	0 K	20K	36K	50K
$C_{L_{req.}}$	.01494	.03262	.0669	.1305	.01494	.03262	.0669	.1305
$C_{L_{gen.}}$	.00845	.00845	.00845	.00845	-.00845	-.00845	-.00845	-.00845
$C_{L_{aft\ wi}}$	.00649	.02417	.05845	.12205	.02239	.04107	.07535	.13895
α aft wing	.54°	1.542°	3.24°	6.76°	1.242°	2.28°	4.18°	7.72°
$C_{D_{aft\ wing}}$	0	.00028	.00161	.0075	.00024	.00081	.00274	.0095
$C_{D_{body\ \&\ gen}}$	.0214	.0214	.0214	.0214	.0214	.0214	.0214	.0214
C_D	.0214	.0217	.0230	.0289	.0216	.0227	.0214	.0309

M_o 3.5								
	ROLLED				UNROLLED			
Alt.	0	20K	36K	50K	0 K	20K	36K	50K
$C_{L_{req.}}$	.01102		.0491	.0960	.01102	.0240	.0491	.0960
$C_{L_{gen.}}$	.0173	see	.0173	.0173	-.0173	-.0173	-.0173	-.0173
$C_{L_{aft\ wing}}$	-.0063	TABLE	.0318	.0787	.0283	.0413	.0664	.1133
aft wing	-.416°	I-1	2.1°	5.19°	1.87°	2.72°	4.39°	7.48°
$C_{D_{aft\ wing}}$	.00005		.00056	.00356	.00046	.00098	.00254	.0075
$C_{D_{body\ \&\ gen.}}$	.02225		.02225	.02225	.02225	.02225	.02225	.02225
C_D	.0223	.02225	.02281	.02581	.02271	.02323	.02479	.02975

CALCULATION OF PERFORMANCE OF A THREE SHOCK SYSTEM M_{DP} 4.0

APPENDIX II

For this system the throat height was assumed to be one inch, giving the schematic shown in Fig. 11 with values as shown in Fig. 12. This gave a diffuser chord of 27 inches, an aft wing chord of 27 inches, and a total chord of 54 inches or 4.5 feet. The wing loading was again assumed to be 200 lb./ft.^{2}. The engine span was taken as 12 ft. with the same size body, making the actual wing span 14.76 ft. and the aspect ratio 3.28. It was again assumed that the missile could be rolled at cruise speed. The effect of restricting this roll was not considered since it was shown to be small in Appendix I.

The calculations were made in the same manner as Appendix I, using the same assumptions. For speeds of M_o 3.5 and below, Lines 1 and 3 through 12 of Appendix I were used. Line 2, the $^{P}T_{2/P_o}$ for this diffuser as shown in Fig. 13, with the Θ_o as given in that figure, is given in Table II-1. As before, an altitude of 20,000 ft. was used for computations below cruise speed. These computations were made in Table II-1, with line numbers corresponding to the line numbers of Appendix I.

M_o 4.0 values were computed using minimum fuel flow. These values are given in Short Table II-2, which was extended in order to show the cruise condition at various altitudes. The C_L and C_D of the generator (Lines 32 and 33) are shown in Fig. 13, and the total C_D and C_F (Lines 39 and 24) are shown in Fig. 14. It should be noted that due to the relatively thicker wing, when compared to the burner height; a larger ϵ was available which gave a $C_{f_{max}}$ at M_o 4.0 of

1.596. This C_f was limited very slightly by wing size, and was found to be 99.7% of C_f optimum. As in Appendix I it can be seen that C_F is well above C_D.

TABLE II-1

CALCULATION OF PERFORMANCE OF A THREE SHOCK SYSTEM M_{DP} 4.0

M_o	1.5	1.75	2.2	2.6	3.0	3.5	Line
P_{T_2}/P_o	3.26	4.66	8.95	16.32	31.4	62.1	2
P_{T_3}/P_o	2.67	3.82	8.00	15.00	29.3	59.0	13
C_f	.89	1.02	1.193	1.32	1.46	1.533	14
ϵ	1.08	1.25	1.75	2.35	4.41	6.64	15
$12A_e$	3.21	3.71	4.8	5.8	9.875	10.0*	16
$12A_{NT}$	2.965	2.965	2.74	2.47	2.24	1.509*	12.5
F_e/P_o	.587	.964	2.18	4.08	8.0	11.37	17
C_{F_e}	.0828	.10	.143	.1913	.282	.2945	18
δ_{t_2}	1.497	2.14	4.11	7.5	14.41	28.3	19
$\sqrt{\theta t_2}$	1.119	1.179	1.304	1.425	1.555	1.725	20
$\dot{w}$	5.3	7.19	12.48	20.85	36.7	65.4	21
C_{F_o}	.0399	.0465	.064	.0904	.1381	.212	23
C_F	.0429	.0535	.079	.1009	.144	.0825	24
$\Theta_{o_{low}}$	8.95	10.5	6.0	3.9	8.0	3.4	25
$C_{L_{low}}$	.1395	.1275	.0533	.0283	.0493	.01787	26
$C_{D_{low}}$	.0223	.024	.0056	.00193	.0070	.00105	27
Θ_{lip}	0	0	5^o	10^o	15^o	22.5^o	28
Θ_{chord}	0	0	.4/54	.6/54	.8/54	1.2/54	29
$C_{L_{lip}}$	0	0	-.0007	-.0016	-.003	-.0052	30
$C_{D_{lip}}$	0	0	.00006	.00029	.0008	.00228	31
$C_{L_{gen}}$	.1395	.1275	.0526	.0267	.0462	.0125	32
$C_{D_{gen}}$	.0223	.024	.00568	.00222	.00775	.00333	33
$C_{L_{req.}}$	.1305	.0961	.0608	.0435	.05262	.0240	34

TABLE II-1 (CONT.)

M_o	1.5	1.75	2.2	2.6	3.0	3.5	Line
$C_{L_{aft\ wing}}$	-	-	.0082	.0168	-	.0115	35
$\alpha_{aft\ wing}$	-	-	$.4^o$	1.2^o	-	1.2^o	36
$C_{D_{aft\ wing}}$	-	-	.00004	.0002	-	.0002	37
$C_{D_{body}}$	.01351	.01309	.01264	.01209	.01152	.01086	38
$C_{D_{tot}}$	.03576	.03709	.01836	.01451	.01927	.01441	39

SHORT TABLE II-2

$M_o = 4.0$ $T_2/T_o = 115.0$ $A_e = 10.0$

Alt.	0 K	20K	36K	50K
T_{T_3}	2720	2419	2179	2179
T_{T_3}/T_{T_2}	1.25	1.288	1.33	1.33
$\phi(M_3)$	.0459	.0472	.0488	.0488
M_3	.227	.231	.235	.235
$\frac{P_{T_2}}{P_3}/1+\gamma M_3^2$	.968	.967	.966	.966
P_{T_2}/P_{T_3}	1.005	1.006	1.007	1.007
12 A_{NT}	1.30	1.321	1.342	1.342
P_{T_3}/P_o	114.2	114.1	114.0	114.0
C_f	1.598	1.597	1.596	1.596
ϵ	.77	.757	.745	.745
F_e/P_o	19.8	20.08	20.35	20.35
C_{F_e}	.393	.399	.404	.404
δ_{t_2}	115.0	52.8	25.8	13.21
$\sqrt{\Theta_{t_2}}$	2.05	1.901	1.781	1.781
$\dot{w}$	232.2	115.0	60.0	30.7

SHORT TABLE II-2 (CONT.)

Alt.	o K	20K	36K	50K
C_{F_o}	.302	.302	.302	.302
C_F	.091	.097	.102	.102
$C_{L_{req.}}$	.00845	.0184	.03775	.0736
$C_{L_{gen}}$	.00725	.00725	.00725	.00725
$C_{L_{aft\ wing}}$	.0012	.01115	.0305	.06635
$\alpha_{aft\ wing}$	-	1.23^o	3.385^o	7.35^o
$C_{D_{aft\ wing}}$	-	.00024	.0018	.0086
$C_{D_{gen}}$	.00464	.00464	.00464	.00464
$C_{D_{body}}$	.0102	.0102	.0102	.0102
$C_{D_{tot}}$	.01484	.01508	.01664	.02344

LOSSES CONSIDERED IN THE CALCULATION OF THE TOTAL PRESSURE RECOVERY

APPENDIX III

The losses considered in the computation of the total pressure recovery were: oblique shock losses in the convergent section, normal shock at the throat, boundary layer build-up in the convergent section, skin friction in the throat, and subsonic diffuser losses. The oblique shock losses were minimized by the method of Oswatitsch, and taken into account as $^{P}T_{1}/P_{T_{O}}$ in Figs. 3 and 12. The normal shock losses at the throat were minimized by the isentropic section of the supersonic diffuser, since this section reduces the flow Mach number so that it approaches Mach 1.0 just prior to the normal shock.

The boundary layer build-up in the convergent section is controlled in two ways. First, the boundary layer bleed in Fig. 6 of the original proposal will reduce losses on the upper surface of the convergent section. Second, wind tunnel experimentation has shown that the boundary layer on the lower surface can be minimized by holes drilled at an angle in the lower surface. These holes are positioned so that the number exposed to the flow will be increased in proportion to the tendency for the boundary layer to grow as the lower lip is extended. It has been demonstrated that this procedure will reduce these losses to negligible values. It should also be noted that the boundary layer bled in Fig. 6 is used for burner area cooling.

Skin friction losses in the throat are incurred throughout the length of the constant area throat required to reduce the flow to subsonic speed. This

loss can be minimized by minimizing the required throat length. This length is made up of two values; a "lost length" of approximately one hydraulic diameter in front of the beginning of the normal shock and a length equal to the "length" of the normal shock. The latter length approaches zero as the Mach number before the normal shock approaches 1.0. This theory has been partially confirmed in a wind tunnel and an average value of skin friction has been found to be .0010 to .0015. Thus the constant area throat required can be reduced to one hydraulic diameter and the friction loss reduced to a negligible value.

The subsonic diffuser losses can be minimized by the use of the optimum expansion angle in the diffuser. This was done and a pessimistic efficiency of .90 was assigned.

This theory of a required constant area throat length that is related to the Mach number before the normal shock was then applied to the oblique plus normal shock diffusers. The Mach number before the normal shock of the one, two, and three oblique shock systems was taken from ref. 6. If it is assumed that the throat length is related to this Mach number, M_t, as shown in Fig. III-1 and that the throat height is one inch, with an assumed coefficient of skin friction, C_{sf}, of .0015; then a total pressure loss due to skin friction in the throat can be computed as shown on Fig. III-1. This loss, $\Delta P_{T_1}/P_{T_o}$, was applied to the total pressure recovery curve in ref. 6, and the result shown in Fig. 3. This loss was found to vary from .23% for the proposed configuration to almost 2.85% for a one oblique plus normal shock diffuser operating at Mach 4.0.

The above loss would seem to be negligible; but from the following, it can

be seen that this is not the case:

Consider the loss as a perturbation on the thrust equation for an ideal expansion:

$$F = F_e - F_o \qquad P_e = P_o$$

where: F_o is the inlet momentum, assumed constant (the free stream conditions remain constant)

$F_e = C_f P_c A_t$ is the exit momentum

C_f is the thrust coefficient of exhaust expansion

A_t is the area of the exhaust nozzle throat

$$P_c \approx P_{T_c} = P_{T_o} \left(P_{T_1}/P_{T_o}\right) \left(P_{T_2}/P_{T_1}\right) \left(P_{T_3}/P_{T_2}\right)$$

P_{T_2}/P_{T_1} was assumed to be .90, and P_{T_3}/P_{T_2} a constant

Thus it can be seen that F_e is proportional to .90 $\Delta P_{T_1}/P_{T_o}$.

Assume a reasonable relationship between F_e and F_o for the cruise condition, say: $F_o = 5/6\ F_e$

therefore: $F = 1/6\ F_e$

$$\frac{\partial F}{\partial \left(P_{T_1}/P_{T_o}\right)} = (6)(.90)\ \Delta P_{T_1}/P_{T_o}$$

Thus the loss in net thrust for the above range of $\Delta P_{T_1}/P_{T_o}$ is actually 1.24% for the proposed configuration to 15.4% for the oblique plus normal shock diffuser.

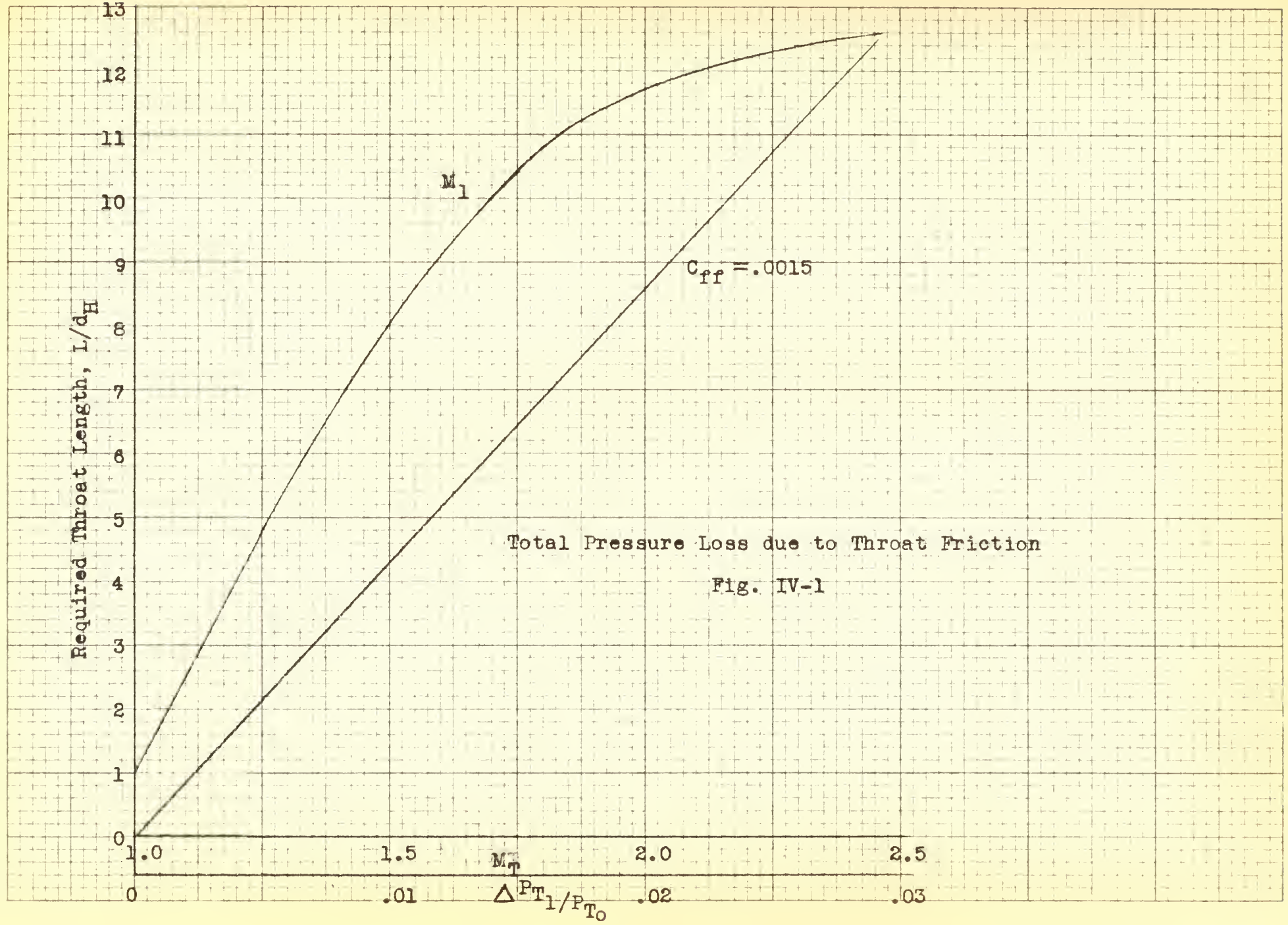

Total Pressure Loss due to Throat Friction

Fig. IV-1